Geological Association of Canada Short Course Notes Volume 13
Dynamic Processes in Magmatic Ore Deposits and their Application to Mineral Exploration
R.R. Keays, C.M. Lesher, P.C. Lightfoot, and C.E.G. Farrow, eds.

Thermal and Fluid Dynamics of Komatiitic Lavas Associated with Magmatic Fe-Ni-Cu-(PGE) Sulphide Deposits

David A. Williams[1], **Ross C. Kerr**[2], and **C. Michael Lesher**[3]

[1]Planetary Geology Group, Department of Geology, Arizona State University, Box 871404, Tempe, Arizona 85287-1404, USA

[2]Research School of Earth Sciences, The Australian National University, Canberra, ACT 0200, AUSTRALIA

[3]Mineral Exploration Research Centre and Department of Earth Sciences, Laurentian University, Sudbury, Ontario P3E 2C6, CANADA

INTRODUCTION

The most important examples of magmatic ore deposits in volcanic rocks are Fe-Ni-Cu-(PGE) sulphides associated with Archean and Proterozoic komatiitic lava channels (Lesher, 1989). Komatiite-hosted ores contain ~25% of the world's nickel sulphide resource (≥ 0.8% Ni), including significant amounts of copper and platinum group elements (Ross and Travis, 1981). Field, experimental, and theoretical studies of komatiite lavas (e.g., Nisbet, 1982; Lesher et al., 1984; Huppert et al., 1984; Huppert and Sparks, 1985a,b; Jarvis, 1995; Greeley et al., 1998; Williams et al., 1998) suggest that they had thermal and physical characteristics that made them particularly capable of thermally eroding their substrates. Because thermal erosion is considered to have played a fundamental role in the formation of komatiite-hosted sulphide deposits (Lesher, 1989; Lesher and Campbell, 1993), understanding the physical dynamics of komatiitic lavas is essential to understanding the dynamics of sulphide generation and segregation processes in high temperature, volcanic ore-forming systems.

The purpose of this chapter is to review the thermal and fluid dynamics of komatiitic lavas as they relate to the formation of magmatic sulphide deposits. This review includes discussion of 1) the physical properties of komatiitic liquids, as inferred from field and petrologic studies, 2) the assumptions required to extend this information to the study of komatiitic lava emplacement, 3) the fluid dynamics of komatiitic lavas, in terms of their physical behavior as lava flows in their emplacement environment(s), 4) the thermal characteristics of komatiitic lavas, with an emphasis on convective heat transfer and the role of thermal erosion and lava contamination, 5) the application of energy conservation to model cooling-limited flow emplacement, and 6) the application of our analytical/numerical computer model to evaluate the role of thermal erosion in komatiitic flow emplacement at the Kambalda and Perseverance deposits in the Norseman-Wiluna greenstone belt of Western Australia and the Katinniq deposit in the Cape Smith belt of northern Québec. These three localities represent endmembers in terms of flow rate, lava composition, and nature and composition of substrate relevant to the emplacement of komatiitic lava flows. We conclude this chapter with a discussion of the relationships between komatiites and their associated sulphides, and suggest a list of outstanding questions as indicators for future research.

PHYSICAL PROPERTIES OF KOMATIITES

Komatiites are high magnesium lavas that formed primarily in Archean greenstone belts, but that also rarely occur in younger volcanic terrains (see Arndt and Nisbet, 1982 for a thorough overview). They are characterized by very high MgO contents (18-32 wt%: Table 1), very low SiO_2 contents (48-44 wt%), and very low incompatible element contents (0.6-0.3 wt% TiO_2), and are therefore interpreted to have been derived by a high degree of partial melting of the mantle (see Herzberg and O'Hara, 1998 for an overview). Physically, these compositions are consistent with very high liquidus (and potentially eruption) temperatures (1360-1640ºC) and very low dynamic viscosities (0.1-2 Pa·s) (Fig. 1, Table 2). As a consequence, komatiites are interpreted to have erupted very rapidly, to have formed highly mobile, channelized flows that traveled great distances (Lesher et al., 1984; Barnes et al., 1988; Hill et al., 1995), and to have been capable, when channelized, of

thermally eroding their substrates (Nisbet, 1982; Huppert et al., 1984; Lesher et al., 1984; Huppert and Sparks, 1985a; Jarvis, 1995; Williams et al., 1998). They are also interpreted to have had very low thermal conductivities (Fig. 2; similar to lunar lavas: Murase and McBirney, 1970; 1973), which would have the effect of greatly reducing heat loss and greatly enhancing long distance flow due to the insulating effects of upper surface crusts. Several recent studies have suggested that *some* komatiites may have contained significant amounts of water (e.g., Parman et al., 1997; Stone et al., 1997), which would have reduced their liquidus temperatures, decreased their viscosities, and reduced their heat capacities. However, it is likely that most komatiites contained little water (Arndt et al., 1998), and so we treat them here as essentially anhydrous. The importance of these physical properties will become clear in later sections where we discuss the fluid dynamic and thermal behavior of komatiitic lava flows, which we utilize in our mathematical model of komatiitic flow emplacement.

ASSUMPTIONS

Modeling the emplacement of komatiitic lava flows, which have never been observed historically, requires many assumptions about their physical and compositional nature and the environments into which they flowed. Thus, model results can be interpreted only as long as the assumptions are valid. As we shall see, some assumptions are justified based upon inferences of their physical behavior as described in Section 2. For example, we will show that the turbulent nature and great thermal erosion potential of komatiites are reasonable assumptions based on the physical properties (i.e., high-temperature, low-viscosity) of komatiitic liquids. Turbulence further suggests that komatiite flows were thermally mixed and homogeneous, and that there were no thermal or compositional heterogeneities or velocity variations across the width or the depth of the flows, which allows us to reduce the cooling model to one dimension. In addition, we assume volume (i.e., flow rate) conservation, so that komatiite flows that erupted as single flow units underwent flow thickness increases during flow velocity decreases. However, in contrast to assumptions about turbulence, assumptions about the behavior of surficial crusts are poorly understood in these lavas. This is due to the lack of easily identifiable crusts in the heavily altered Precambrian komatiites. We assume that surface crusts formed quickly and that flows were completely covered, and although crusts should have been continually broken up by turbulence, entrained, and remelted (Keszthelyi and Self, 1998), they would quickly reform, thus providing a stable "insulating boundary."

Other assumptions, primarily those based on the environment of flow emplacement (e.g., sea water temperature, ground slope, nature of the substrate, presence and degree of preservation of embayments), are much less well constrained. For example, pillow basalts overlying and underlying komatiites at Kambalda suggest submarine emplacement. We assumed that these submarine komatiitic eruptions occurred at a depth of ~1 km below sea level, and that the lavas flowed over a flat, homogeneous, unobstructed Archean sea floor with a slope of 0.1% (similar to that assumed for CRB emplacement: Self et al., 1996, 1997). This assumption does not consider the influence of local topographic variations, which may occur with some substrates. We will show that as the complexity of the substrate increases (e.g., greater heterogeneity, lower degrees of consolidation), the greater number of assumptions are required to model thermal erosion and lava emplacement. For example, the complex substrates at Kambalda (a thick sequence of massive- to pillowed-basalts overlain by thin, unconsolidated, water-saturated interflow sediments), Perseverance (a thick sequence of felsic tuffs of unknown degree of consolidation), and Katinniq (a thick gabbroic sheet flow overlain by a thick sequence of semi-pelitic sediments) require additional assumptions to model, as we will discuss later.

FLUID DYNAMICS OF KOMATIITES

The exceptionally low viscosity of komatiite lavas results in a fluid dynamic behavior atypical to that of modern lavas. Consider a theoretical komatiite lava flow (Fig. 3) of initial thickness h and width w that is erupted at some eruption temperature T_0 on a shallow-sloping ocean floor[1] at ambient temperature T_a. For a flow moving at flow velocity u, it is possible to determine the flow regime using the

[1] The evidence for submarine emplacement of komatiite lava flows comes primarily from field evidence, in which (as mentioned above) most komatiites are associated with pillow basalts stratigraphically above and below them. In addition, individual komatiite flow units are often interlayered with dark, fine-grained sediments (Lesher et al., 1984; Barnes et al., 1988; Hill et al., 1990, 1995) interpreted to represent deep marine environments.

Reynolds number (Re), which represents the ratio of inertial to viscous forces in a moving fluid

$$Re = \frac{\rho_b h u}{\mu_b} \quad (1)$$

in which h is a characteristic length, in this case assumed to be the flow thickness (m), u is the flow velocity (m/s), μ_b is the bulk viscosity of the lava (i.e., the viscosity of the liquid plus any solid crystals entrained in the flow) (Pa s), and ρ_b is the bulk density of the lava (kg/m^3). For confined pipe, tube, or open channel flows, Re < 500 corresponds to laminar flow, Re > 2000-2300 corresponds to turbulent flow, and 500 < Re < 2000 corresponds to a transitional regime that can include either laminar or turbulent flow, depending upon the properties of the fluid[2] and external conditions. As indicated in Figure 4, for reasonable choices of flow thickness and flow velocity, the low viscosity of komatiite lavas suggests they would have been emplaced as turbulent flows.

As also indicated in Fig. 4, the magnitude of the Reynolds number is strongly dependent upon the viscosity of the fluid and the flow thickness or flow rate of the lava. The (two-dimensional) flow rate of the lava Q (m^2/s) is expressed as the product of the flow velocity u (m/s) and the flow thickness h (m). For a lava flow of given composition and viscosity flowing down a shallow slope, it is possible to calculate the flow velocity using the following equation (modified from Jarvis, 1995)

$$u = \sqrt{\frac{4g\,\Delta\rho\,\sin(\psi)}{\rho_b \lambda}} \quad (2)$$

in which g is gravitational acceleration (m/s^2), $\Delta\rho$ is the density difference between the lava and the overlying fluid (kg/m^3), ψ is the slope of the ground (^{o}), and λ is the dimensionless friction coefficient for turbulent pipe flows given by Kakaç et al. (1987)

$$\lambda = \left(0.79\,\ln(Re) \pm 1.64\right)^{\pm 2} \quad (3)$$

Equations (1), (2), and (3), when solved iteratively, give the flow velocity, flow rate, and Reynolds number for a turbulent lava flow of any given thickness, viscosity, and density moving down a given ground slope. Furthermore, as can be inferred from Fig. 4, increasing viscosity of the flow will decrease Reynolds number, increase friction coefficient, and thus decrease the flow velocity of the lava. Assuming a constant flow rate during lava emplacement (and conservation of volume in a lava flow), a decrease in flow velocity must be compensated for by an increase in flow thickness. This means that lava flows become thicker as they slow down, all else being equal. This effect is probably minor for all but the thickest komatiite flows, as other factors (e.g., viscosity changes, flow shape, topography) will have greater affects. Note that this concept is different than the process of "inflation" that is observed in modern Hawaiian basalt lavas, in which thin, relatively stationary flows increase in thickness due to injection of lava under a thin crust, followed by slow advancement of the flow by "budding" or breakouts of pahoehoe toes (e.g., Walker, 1991; Hon et al., 1994). Although inflation has been proposed to have occurred to a minor degree in some komatiites (e.g., Lesher et al., 1984), with all things equal inflation at flow fronts reduces horizontal flow rates and therefore diminishes the potential for thermal erosion.

In summary, the above discussion outlines the important physical factors that must be understood to consider the emplacement and erosional potential of komatiitic lavas. For any given flow rate and ground slope, higher MgO and lower SiO_2 komatiitic liquid compositions result in higher temperature, lower viscosity, potentially turbulent flows emplaced on or near the surface, relative to modern tholeiitic basalt lavas which produce lower temperature, higher viscosity, laminar flows. Next, we turn our attention to the implications of these properties on cooling of komatiitic liquids during flow emplacement.

HEAT TRANSFER IN KOMATIITES

The factors that control heat transfer (i.e., cooling) in a lava flow include such intensive parameters as flow rate, viscosity, vesicularity, volatile content, eruption temperature, composition, and presence and nature of a surface crust, as well as such extensive parameters as eruption environment (i.e., subaerial, subaqueous, or in a vacuum) and slope and topography of the substrate (e.g., Nichols, 1939; Shaw and Swanson, 1970; Walker, 1973; Hulme, 1974; Malin, 1980;

[2] It is important to emphasize that there has never been a historic komatiite eruption, so much of this analysis is based on theoretical and laboratory studies (e.g., Huppert et al., 1984; Huppert and Sparks, 1985a).

Crisp and Baloga, 1990). As we have seen, most komatiite lavas are inferred to have been anhydrous, hot, low viscosity, turbulent flows that were very different from modern lavas. We can quantify the effects of these physical properties based on our understanding of the emplacement of modern lavas and low-viscosity analog substances. Furthermore, through field studies we can infer the nature of the emplacement environment for komatiitic lavas. Thus, it is possible to determine the types and magnitudes of the major heat loss mechanisms that would have affected komatiitic lava flows. These heat loss mechanisms cause a decrease in lava temperature (T) as a function of time (t) since cooling began and distance (x) of the flow downstream from its source vent. Unlike modern, laminar basaltic flows, which cool primarily through conduction to the surroundings, a low viscosity, turbulent komatiitic flow with a thermally mixed interior would have undergone strong convective heat transfer. As indicated in Fig. 3, in the case of submarine komatiite lavas, this convection would have:

1) Transferred heat to the base of a crust that quickly formed against the exposed surfaces of the flow, where this crust was maintained at the lava solidus temperature.

2) Transferred heat to the sea floor, which underwent thermal erosion if lava temperature T was greater than the ground melting temperature T_{mg}.

In addition, conductive heat transfer would have occurred through the growing upper surface crust. Each of these mechanisms is discussed below.

Convective Heat Transfer Coefficients

The convective heat flux from the komatiite lava to a surface can be expressed in terms a convective heat transfer coefficient (h_T: see e.g., Holman, 1986). Heat transfer coefficients (h_Ts) are used in mechanical engineering to estimate turbulent and laminar heat transfer for fluids like air in ducts, water in pipes, or industrial oils in engines, all of which can have heat transfer conduits with various geometries. Because natural geologic environments are fundamentally different from the well-controlled laboratory experiments in which most h_Ts were developed, it is difficult to apply experimentally- or empirically-determined h_Ts to lava flows. In particular, most h_Ts were developed for fluids with constant flow properties (i.e., thermal conductivity, Reynolds number, Prandtl number) that: 1) undergo small temperature changes during flow, 2) vary in temperature only slightly from the temperature of the conduit wall, and/or 3) have no viscosity variation between the fluid interior and the fluid at the conduit wall. In contrast, komatiite lava flows: 1) undergo large temperature changes during emplacement that result in significant variations of flow properties with flow distance, 2) have large temperature differences between the lava flow and the ambient environment, and 3) have a large viscosity variation between the komatiite flow interior and the melted substrate at the tube/channel floor. Thus, any attempt to model convective heat transfer by komatiitic lavas is crude at best, and it is important to choose the best h_T for modeling a given scenario of komatiitic lava emplacement.

There are many h_Ts available for turbulent and laminar flow, but perhaps the best available equation for our purposes is given by (e.g., Kakaç et al., 1987)

$$h_T = \frac{0.027 k_{eff} Re^{0.8} Pr^{0.33}}{h} \left(\frac{\mu_b}{\mu_g} \right)^{0.14} \qquad (4)$$

in which k_{eff} is the effective lava thermal conductivity (J/m/s/ºC) in the thermal boundary layer between the fluid and the conduit wall and μ_g is the viscosity of the fluid (i.e., melted substrate) in contact with the conduit wall. The variable Pr is the lava Prandtl number, the dimensionless ratio of momentum diffusion to heat diffusion in the lava, which is given by:

$$Pr = \frac{c_b \mu_b}{k_{eff}} \qquad (5)$$

in which c_b is the lava bulk specific heat (J/kg/ºC). The viscosity ratio term (μ_b/μ_g) in Equation (4) has been experimentally determined for $0.0042 < (\mu_b/\mu_g) < 9.75$, which roughly covers the range of variation in fluid properties found in komatiitic lavas. Although Equation (4) has been calibrated for only high Reynolds numbers ($Re \geq 10^4$), we believe that it provides a reasonable estimate of convective heat transfer for confined (i.e., tube- or channel-fed) turbulent komatiitic lava flows that have thermal/rheological properties that vary during emplacement.

Convective Heat Transfer to the Upper Surface Crust

Heat will be transferred by convection from the turbulent komatiite lava interior to an upper surface crust that forms when the hot lava is quenched in contact with overlying cold sea water. Because a comparison of the convective heat flux in the lava with the convective heat flux off the upper surface due to cold sea water (Williams, 1998) shows that the sea water has a greater capacity to remove heat from the lava by convection than the lava has the capacity to deliver heat to the lava/sea water interface, it is clear that a crust should form quite quickly (on the order of seconds) on the top of a submarine komatiitic flow. This occurs at a contact temperature at the lava/sea water interface of ~90ºC, which is far below the glass transition temperature of basalt (~730ºC: Ryan and Sammis, 1981) and presumably also less than that for komatiite. Thus, unless the turbulence of the lava breaks up the crust continuously on a timescale less than the time required to form the crust, which seems unlikely, some type of insulating crust should exist on the upper surface of a submarine komatiite lava flow (equivalent to a tube-fed turbulent flow?). Equation (4) can be rewritten to give the convective heat transfer to the base of the upper surface crust by letting k_{eff} be the thermal conductivity in the upper thermal boundary layer between the lava interior and the base of the crust (at the lava solidus temperature T_{sol}) and by letting μ_g be the viscosity of the base of the lava crust, which is a function of lava temperature. Equation (4) is multiplied by the temperature difference between the turbulent lava interior and the base of the crust to convert the heat transfer coefficient to heat flux ($J/m^2/s$).

Convective Heat Transfer to the Ground

In like manner, Equation (4) can be adapted to estimate the convective heat transfer from the turbulent lava interior to the flow base in contact with some substrate, simply by letting k_{eff} be the thermal conductivity in the lower thermal boundary layer between the lava interior and the base of the flow (at the ground melting temperature T_{mg}) and by letting μ_g be the viscosity of the base of the lava flow. Once again, Equation (4) is multiplied by the temperature difference between the turbulent lava interior and the base of the flow to convert heat transfer coefficient to heat flux ($J/m^2/s$). An additional factor must be considered when the lava temperature T is greater than the ground melting temperature T_{mg}, namely the potential for substrate melting (thermal erosion). This process is thought to be the key to understanding the formation of certain komatiite-hosted magmatic sulphide deposits, which will be discussed further below.

Conductive Heat Transfer through the Crust

The final mechanism of heat transfer we will discuss here is conduction through a growing surface crust. As we indicated in Section 5.2, initially the molten lava is in contact with cold sea water, but almost immediately the lava quenches to glass and forms a thin crust with a brittle upper surface and a more ductile lower surface (viscosity similar to molasses) that is maintained at the lava solidus. The term for the conductive heat flux ($J/m^2/s$) through the crust depends upon the thermal conductivity (k_c) of the solid crust (i.e., the ability to transmit heat through the solid crust), the thickness (h_c) of the crust (i.e., the distance across which heat must be transmitted), and the temperature range between the base of the crust (T_{sol}) and the top of the crust (T_c)

$$\frac{k_c}{h_c}\left(T_{sol} \pm T_c\right) \qquad (6)$$

During lava emplacement, the crust thickens until the heat transfer by conduction through the crust is equal to the convective heat transfer to the crust from the underlying turbulent lava flow. Thus, the main influence of the crust on the lava flow is to insulate it from the more rapid heat loss one would expect from an uncrusted flow, which in turn allows the lava flow to travel farther than if the flow was uncrusted. As we indicated in Section 2, one assumption with this argument is that a thin, continuous crust can be maintained on top of a turbulent flow. In fact, turbulence might be expected to continually breakup, entrain, and reform the crust. Fragmental, continuously breaking and reforming crusts are less effective insulators of heat compared to flows with smooth, unfractured crusts (e.g., terrestrial pahoehoe flows: Keszthelyi and Self, 1998). Field studies of Archean and Proterozoic komatiites (e.g., Arndt et al., 1979) indicate that both types of crusts may have existed, and thus further study of the relationship between type of crust and emplacement style is warranted.

In summary, in contrast to modern basaltic flows which cool mostly by conduction, hot, low-viscosity, turbulent komatiites must have cooled mostly by convection from the hot flow interior to the base of

the upper crust and to the base of the flow in contact with the substrate. Although convection from the lava is expected to result in rapid heat loss from the flow, the rapid formation of a thin crust at the lava/sea water interface may act as an effective insulator of heat, enhancing the potential for long-distance flow in lava tubes. In addition, because komatiites could have erupted at temperatures far above the melting temperatures of most substrate lithologies, the potential for thermal erosion is very great. We now will discuss the role of thermal erosion in komatiitic lava flow emplacement.

THERMAL EROSION AND ASSIMILATION OF SUBSTRATE

As a consequence of the probable high temperatures, low viscosities, turbulent flow and convective heat loss regimes of komatiite lavas, Nisbet (1982) suggested that they might be capable of thermally eroding their substrates/wall rocks. Thermal erosion is a geologic process that involves the breakup and removal of substrate by hot flowing lava. This process may include both thermal ablation (i.e., melting) of consolidated and unconsolidated substrate due to heating by the lava and physical degradation (i.e., mechanical erosion) of unconsolidated or partly consolidated material and melt due to shearing or plucking by the moving lava, followed by partial or complete assimilation of melted substrate into the liquid lava. Thermal erosion has been inferred to have had a role in the formation of terrestrial lava tubes for many years (e.g., Greeley, 1971a,b, 1972; Cruikshank and Wood, 1972; Greeley and Hyde, 1972; Swanson, 1973; Peterson and Swanson, 1974; Wood, 1981; Coombs et al., 1990; Peterson et al., 1994; Greeley et al., 1998), and has recently been measured (using geophysical techniques) in active tubes with laminarly-flowing lavas in Hawaii (Kauahikaua et al., 1998). It is also thought to have occurred during the emplacement of carbonatite lavas at Oldoinyo Lengai, Tanzania (Dawson et al., 1990) and industrial sulphur flows (Greeley et al., 1990), and played a role in the formation of some extraterrestrial lava channels such as the lunar sinuous rilles (Hulme, 1973, 1982; Head and Wilson, 1981), some Martian lava channels (Carr, 1974; Cutts et al., 1978; Baird, 1984; Wilson and Mouginis-Mark, 1984), and some Venusian canali (Head et al., 1991; Baker et al., 1992; Komatsu et al., 1993; Komatsu and Baker, 1994; Bussey et al., 1995). The role of thermal erosion in the emplacement of komatiites was investigated in the landmark work of Huppert et al. (1984) and Huppert and Sparks (1985a,b), and further refinements to their work have been done by Jarvis (1995) and Williams et al. (1998). As we shall see, thermal erosion is considered to be a requirement for the formation of some magmatic sulphide deposits.

For the case of submarine komatiite flows described in this chapter, it is possible to calculate the thermal erosion rate of the substrate for different circumstances of lava emplacement. For example, the one-dimensional lava thermal erosion rate u_m (m/s) into the substrate at any given distance x from the eruption source is given by

$$u_m = \frac{h_T\left(T \pm T_{mg}\right)}{E_{mg}} \tag{7}$$

in which h_T (J/m^2/s/^{o}C) is the convective heat transfer coefficient from the lava to the substrate (see Section 5.3), T_{mg} is the effective melting temperature of the substrate (^{o}C), and E_{mg} is the energy required to remove the substrate (J/m^3). A value of T_{mg} for any given substrate can be chosen along with the appropriate value of substrate viscosity μ_g to maximize the heat flux to the substrate, and thus maximize erosion rate. This erosion rate u_m can be multiplied by specific values of elapsed time t since emplacement began (s) to give the erosion depth d_m (m) into the substrate

$$d_m = u_m \cdot t \tag{8}$$

Because the volume flux or two-dimensional flow rate Q(x) (m^2/s) of the lava increases with distance with the addition of material by thermal erosion, the degree of lava contamination as a volume fraction of the lava S(x) can be determined from the ratio of the volume flux at any given distance to the initial volume flux Q_0

$$S\left(x\right) = 1 \pm \frac{Q_0}{Q\left(x\right)} \tag{9}$$

in which each side of Equation (9) is dimensionless and the volume flux is given by

$$Q\left(x\right) = Q_0 + \int_0^x u_m dx \tag{10}$$

and Q_0 is simply the initial volume flux. Note that the addition of material to the flow by thermal

erosion also causes a theoretical increase in flow thickness.

In addition to calculating the erosion rate and erosion depth into the substrate and the degree of contamination of the lava, these parameters can be used to determine the geochemical evolution of the lava during emplacement. Specifically, using Equation (9) in conjunction with the appropriate lava and substrate major oxide compositions and mass balance equations, the lava composition can be adjusted for the addition of substrate material by thermal erosion. Because heat loss due to melting of the substrate must also be accompanied by crystallization of olivine (the primary rheology-altering silicate phase to crystallize during turbulent emplacement from all but the most strongly-contaminated komatiites), it is possible to calculate the effects of olivine crystallization on the heat budget and on magma composition. By using olivine-liquid partition coefficients (Beattie et al., 1991, 1993; Kennedy et al., 1993) in conjunction with stoichiometric constraints, mass balance expressions, and estimates of the crystallization rate during cooling, the lava composition may be adjusted for the subtraction of olivine crystals that form during cooling. As a consequence, the residual liquid lava becomes more silicic due not only to the addition of assimilated substrate material, but also due to the removal of Mg and Fe in the olivine that crystallizes during cooling and emplacement. The effects of olivine crystallization can be evaluated in terms of the gain in heat content ($J/m^2/s$) of the flow due to latent heat of crystallization:

$$+ \rho_x h L_x X'(T) \frac{dT}{dt} \qquad (11)$$

in which ρ_x is the crystal density (kg/m^3), L_x is the heat released during formation of solid crystals from the liquid lava (J/kg), and X'(T) is a first-order estimate of the rate of increase in the volume fraction of crystals with decreasing temperature, equal to $\_1/625\ ^oC^{-1}$ (derived from the slope of the olivine liquidus: see fig. 2 in Usselman et al., 1979). The net result is the ability to determine the geochemical evolution of the lava during emplacement, and the evolving composition is used to recalculate important physical properties like viscosity, density, specific heat, and in turn flow velocity, Reynolds number, Prandtl number, heat transfer coefficient, etc. This discussion brings us to the final component of any model of lava flow emplacement, that of conservation of energy in a cooling-limited flow that allows calculation of lava temperature as a function of distance.

CONSERVATION OF ENERGY IN LAVA COOLING

Our goal is to model cooling-limited komatiite lava emplacement by predicting the values of important rheological, fluid dynamic, thermal, and geochemical parameters as a function of time since emplacement began, or as a function of distance from the eruption source. The previous sections have outlined how the lava and substrate compositions, the lava temperature, and the nature of the emplacement environment affect calculations of the important rheological, fluid dynamic, thermal, and geochemical parameters. The final step of the discussion is to describe how these parameters are used to calculate the decrease in lava temperature as a function of distance.

The cooling of all hot fluids must follow the law of energy conservation, in which heat gains are balanced by heat losses. Cooling of lava flows is complicated by the presence of phase changes, most notably the crystallization of solid minerals from the liquid lava, which results in the release (gain) of latent heat (Equation 11). From the discussion of heat loss mechanisms given above, the likelihood of thermal erosion occurring during komatiite flow emplacement, and the release of latent heat, we can list the important heat fluxes ($J/m^2/s$) present in a komatiite lava flow:

Heat content of flow

$$+ \rho_b c_b h \frac{dT}{dt} \qquad (12a)$$

Convective heat transfer to substrate

$$\pm h_T \left(T \pm T_{mg} \right) \qquad (12b)$$

Convective heat transfer to base of crust

$$\pm h_T \left(T \pm T_{sol} \right) \qquad (12c)$$

Convective heat transfer raising melting ground to T

$$\pm \frac{\rho_g c_g h_T \left(T \pm T_{mg} \right)^2}{E_{mg}} \qquad (12d)$$

Heat gain from latent heat of crystallization (Eq. 11)

$$+ \rho_x h L_x X'(T) \frac{dT}{dt} \qquad (12e)$$

in which ρ_g is the density of the melted ground (kg/m^3) and c_g is the heat capacity of the melted ground ($J/kg/^oC$).

By correctly assembling these heat fluxes according to conservation of energy, and by recognizing the relationship between time and distance:

$$\frac{dT}{dt} = u \frac{dT}{dx} \qquad (12f)$$

a first-order ordinary differential equation is produced that calculates the decrease in lava temperature as a function of distance:

$$\rho_b c_b h \frac{dT}{dt} = -h_T(T - T_{mg}) - h_T(T - T_{sol}) - \frac{\rho_g c_g h_T (T - T_{mg})^2}{E_{mg}} + \rho_l h \frac{dT}{dt} L_l X'(T) \qquad (13)$$

Because properties like density, specific heat, flow thickness, flow velocity, and heat transfer coefficient continually change with distance, Equation (13) must be solved numerically at every downflow distance of interest. It is possible to solve Equation (13) using a 4th-order Runge-Kutta numerical method for a constant distance increment (Williams et al., 1998). By choosing a lava eruption temperature and composition to calculate the initial lava properties given in Table 1 and discussed in Sections 4-6, and by using updated values of these properties at each distance increment calculated from Equation (13), the thermal, fluid dynamic, and geochemical evolution of a komatiitic lava flow can be modeled as a function of distance. A version of Equation (13) was first presented in Huppert and Sparks (1985a). However, with the inclusion of the temperature- and composition-dependent properties described above, and also presented in Williams et al. (1998), we believe our model provides a more rigorous estimate of the emplacement and thermal erosion potential of Archean and Proterozoic komatiitic lava flows, within the uncertainties of the initial emplacement parameters (e.g., lava eruption temperature, thickness, composition) and the assumptions of the model, which we discussed in Section 3.

APPLICATIONS

Parameters Controlling Lava Emplacement

A sensitivity analysis of the input parameters and algorithms from the komatiite emplacement and erosion model discussed above has been performed (see Williams, 1998, for a full discussion), and a summary of the effects of individual model parameters on output is given in Table 3. In some cases, flow behavior is straightforward; for example, if flow thickness (i.e., flow rate) or lava MgO content (i.e., temperature) are increased, then model flows travel farther and have higher erosion rates and degrees of contamination at any given distance. In other cases, flow behavior is more complex. For example, superheated lavas[3] flow for longer distances at higher temperatures with higher erosion rates, and attain greater maximum degrees of contamination than non-superheated flows. However, their maximum flow distances are generally less than non-superheated lavas, because the higher contamination results in a faster change in rheology and faster decrease in turbulent flow. Also, a more felsic (i.e., lower melting temperature) substrate does not necessarily have a higher erosion rate than a mafic substrate, because the higher viscosity contrast between the komatiite lava and the felsic substrate tends to reduce heat transfer. However, if the felsic substrate is unconsolidated and hydrous (i.e., contains intergranular water), then thermal erosion may be enhanced by disaggregation of the felsic material by vaporizing intergranular water (see discussion by Williams et al., 1998).

In summary, the results of this analysis suggest that flow rate, lava composition, substrate composition and degree of consolidation (including intergranular and compositional H_2O), eruption temperature, and ground slope are the most important parameters that affect model output, and thus the best estimates possible are required for starting values of these parameters. In particular, the presence of intergranular or compositional water enhances the erodability of some substrates, whereas the presence of a large viscosity contrast between the komatiite lava and the melted substrate reduces the erodability of a substrate,

[3] Because of their very low viscosities, high heat contents, and low thermal conductivities, komatiites are likely to have ascended along P-T trajectories much steeper than the komatiite liquidus and some komatiites may have therefore erupted in a superheated state (Lesher and Groves, 1986).

and this effect is greatest for very felsic substrates. Huppert and Sparks (1985a) predicted that the maximum contamination of komatiite lavas by any substrate would be ~10% for subliquidus emplacement on relatively flat slopes at all flow rates for flow distances up to 100 km, with larger maximum contamination values possible only for longer flow distances and higher flow rates. Our sensitivity analysis suggests that the maximum contamination of komatiite lavas by substrate can be >>10% if the lava was erupted in a superheated state or if thermo-mechanical erosion of an unconsolidated, fine-grained substrate containing a sufficiently large fraction of intergranular water occurred. These concepts are further examined by applying this komatiite emplacement and erosion model to several sites where thermal erosion has been inferred.

Kambalda

The emplacement of high temperature, high MgO komatiite lavas at Kambalda, Western Australia, has been modeled by Williams et al. (1998). Kambalda is the "type locality" for komatiite-hosted magmatic nickel sulphide ores, which are localized in flat-floored, reentrant embayments in the basaltic substrate (Fig. 5). There has been, and continues to be, much debate regarding the origin of these embayments (see review by Lesher, 1989), which have been proposed to represent: 1) volcanic features formed entirely by thermal-mechanical erosion (Huppert et al., 1984; Huppert and Sparks, 1985a), 2) volcanic topographic features modified by thermal-mechanical erosion and deformation (Lesher et al., 1984; Evans et al., 1989; Lesher, 1989), and 3) structural features involving no thermal-mechanical erosion (Cowden, 1988). By using field constraints on flow rates and lava/substrate compositions, Williams et al. attempted to investigate the viability of these hypotheses.

Because Kambalda contains both a thick, consolidated, basaltic substrate and an overlying thin, sulphidic sedimentary substrate, this locality is useful for testing the erodability of these two endmembers. Although it is unknown whether the sulphidic sediment at Kambalda behaved as a consolidated or unconsolidated substrate, Williams et al. (1998) developed models to investigate the erosive potential of both substrates. For a water-saturated, unconsolidated sediment, it was assumed that heat from the flowing komatiite lava caused intergranular sea water in the substrate sediment to boil, vaporize, and expand, fragmenting the sediment. Subsequently, the disaggregated sediment mixed mechanically with the lava (i.e., underwent mechanical erosion) before melting in the lava. Williams et al. (1998) reported that sediment composed of very fine sand-sized particles or smaller (i.e., particle diameter ≤0.125 mm) could have been fluidized in this manner, resulting in enhanced thermo-mechanical erosion of unconsolidated sediments compared to thermal erosion of more consolidated rocks (Fig. 6).

We have redone the modeling of Williams et al. (1998) using a higher (~32%) MgO lava composition for the Kambalda komatiites (Table 2), which we believe was the probable composition of the parental (unfractionated) magma. The key results may be summarized as follows:

1) Model results using field data to constrain the choice of important model parameters (e.g., flow thickness, crust thickness, and lava composition) suggest that thermal erosion is strongly dependent upon the nature and behavior of the substrate.

2) An initially 10m thick komatiite lava flowing over an unconsolidated, hydrous, fine-grained sediment would have produced the observed crustal thicknesses of ~5-20 cm at distances of ~20-60 km from the source, very high thermo-mechanical erosion rates (~20-9 m/day), and a high degree of lava contamination (~12-20%).

3) In contrast, a more consolidated, anhydrous sediment that could not be fluidized would have had much lower thermal erosion rates (~1-0.4 m/day) and degrees of contamination (~3-5%), and lavas would have had crustal thicknesses of ~5-20 cm at longer flow distances of ~90-265 km from the source. A consolidated, anhydrous basalt would have had a thermal erosion rate of ~0.7-0.3 m/day and degrees of contamination of ~3-5%, and lavas would have had crustal thicknesses of ~5-20 cm at longer flow distances of ~115-340 km from the source. Geochemical and isotopic data indicate that komatiite lavas in parts of the host units at Kambalda are locally contaminated up to 2-5% (Lesher and Arndt, 1995).

4) The reentrant embayments at Kambalda are thought to have formed by erosion of deep (~10s m) channels into a flat basaltic sea floor (Huppert et al., 1984) or by erosion of a thin (<5 m) sediment with minor undercutting of basalt within pre-existing topographic features (Lesher et al., 1984). The modeling results indicate that the deep embayments at

Kambalda could have formed by thermal erosion of basalt (Huppert and Sparks, 1985a) only during long duration eruptions (months), whereas only minor erosion of sediment in pre-existing lava channels (Lesher et al., 1984) could have occurred during short duration eruptions (<2 weeks). Although there is local evidence of thermal erosion of basalt at Kambalda (Evans et al., 1989; Lesher, 1989) and although some of the smaller embayments at Kambalda are concave and may have formed by thermal erosion, most are flat-floored (see Gresham and Loftus-Hills, 1981) and appear to represent volcanic topographic features (Lesher, 1989). If so, this suggests that shorter eruption durations were more likely.

Although our model cannot establish unequivocally whether the Kambalda embayments are incised thermal erosion channels or topographic features modified by thermal erosion and deformation, it is clear from the modeling and other field/geochemical studies (Groves et al., 1986; McNaughton et al., 1988; Evans et al., 1989; Frost and Groves, 1989; Lesher and Arndt, 1995) that thermal erosion of sulphide-rich interflow sediment must have occurred at Kambalda. Importantly, this process would have provided S for the generation of the magmatic sulphide deposits (Lesher et al., 1984; Lesher and Campbell, 1993), which we will elaborate on in the Discussion section.

Perseverance

The Perseverance Ultramafic Complex (PUC) is a large, lens-shaped body of olivine adcumulate komatiite overlying a thick substrate of dacitic tuff in the northern part of the Norseman-Wiluna greenstone belt, Western Australia (Fig. 7). The most comprehensive geological description and interpretation was done by Barnes et al. (1988), who interpreted the area as a broad (1-3 km wide), concave submarine thermal erosion channel (~100-150m deep) formed by a thick, high MgO (up to 33%) komatiite lava "river", resulting from a large flow rate eruption(s) of komatiite lava on a scale akin to the lunar maria or the continental flood basalts. The PUC is a challenging locality to model komatiite lava emplacement and thermal erosion in several respects.

First, post-emplacement tectonic deformation and mid-amphibolite facies metamorphism have modified or obliterated most of the igneous structures and textures in the PUC, so that there are no field data to constrain initial lava flow thickness or crustal thickness in the PUC. To model this locality, we are required to assume that the PUC was emplaced in manner similar to nearby komatiite localities, which are compositionally and morphologically similar with channelized sheet flows tens of meters thick and upper chilled margins typically ≥10 cm thick (S.J. Barnes, pers. comm., 1998). For example, the adjacent Rocky's Reward ultramafic unit, which may in fact represent an attenuated tectonic slice off of the bottom of the PUC, is composed of flows ~30-40m thick (S.J. Barnes, pers. comm., 1998), although the initial flow thickness may have been as much as 100m. Thus, we have modeled Perseverance using a range of flow thickness: 10m, 30m, and 100m.

Second, the substrate underlying the PUC is a thick (~150 m) sequence of feldspar-phyric tuffs of dacitic to rhyolitic composition with calc-alkaline geochemical affinities (Barnes et al., 1988; 1995), which is potentially very erodable, but poorly characterized. No sedimentological data (e.g., grain size, porosity, etc.) are available for these metamorphosed tuffs and the size of the groundmass component has not been identified, although the phenocryst component of the tuffs appears to have been coarse sand-sized (S.J. Barnes, pers. comm., 1998). This is probably a maximum grain size, as it is reasonable to assume that both the phenocryst and groundmass components have increased in grain size during the prograde amphibolite facies metamorphism that has occurred in the Perseverance area. It is unknown whether the tuffs represent welded subaqueous pyroclastic flow deposits (e.g., Sparks et al., 1980), or subaqueous unconsolidated pyroclastic fall deposits. It is also unclear what the S source was for the sulphide deposits found at the floor of the embayment. There are several sulphide schist marker beds within the substrate, but their small size would seem to preclude them as the source of the massive sulphide deposit.

Third, the degree of contamination appears to be much greater than at Kambalda further to the south, but is less well constrained. Barnes et al. (1988) reported apparently high levels of lava contamination (later estimated to be ~10-20%: S.J. Barnes, pers. comm., 1997) in the ~30m thick flows at Rocky's Reward and in the Perseverance Mineralized Flows, as well as in the shallow flanking flows in the Perseverance Ultramafic (PU) North area. Barnes et al. (1995) suggested that continued thermal erosion of the thick felsic substrate by komatiite lava would produce these highly contaminated lavas in the central channel as long as komatiite lava remained hot

enough and flowed fast enough to remove substrate. This degree of contamination is much greater than the 2-5% reported at Kambalda (Lesher and Arndt, 1995), presumably because the felsic sediment at Kambalda was much thinner (average 1m), resulting in less contamination (see discussion by Lesher and Stone, 1996; Williams et al., 1998).

Finally, there is some debate regarding the composition of the initial magma. Barnes et al. (1988) reported cumulate olivine compositions exceeding Fo_{95} and inferred that the initial magma contained up to 33% MgO. Nisbet et al. (1993) argued that this would imply excessive mantle potential temperatures and that maximum MgO contents of Archean komatiites were ≤28%. The problem is that magmas with lower Mg contents (and consequently higher Fe contents if derived by partial melting of the same source or by fractional crystallization from the same parent) cannot produce such magnesian olivines. For example, using K_D^{Fe-Mg} = 0.30 and assuming 5% Fe^{3+}, a magma with 33% MgO and 9.4% FeO_{total} would be in equilibrium with $Fo_{95.6}$, but a magma with 28% MgO and 10.4% FeO_{total} would be in equilibrium with $Fo_{94.4}$. Contamination would decrease the Fe content of the magma relative to Mg (as a consequence of contamination and crystallization) and might also increase fO_2 (if the magma incorporated H_2O during assimilation of the tuff, which dissociated and increased fO_2). For example, a contaminated magma with 28% MgO, 9.4% FeO_{total}, and 5% Fe^{3+} would be in equilibrium with $Fo_{94.9}$, whereas a contaminated magma with 28% MgO, 9.4% FeO_{total}, and 10% Fe^{3+} would be in equilibrium with $Fo_{95.2}$. However, this would still require a more magnesian (and presumably uncontaminated and unoxidized) parent. Thus, we have utilized a relatively high (~32%) MgO lava composition for our modeling of Perseverance (Table 1).

Despite these uncertainties and complications, we have attempted to model komatiite lava emplacement at Perseverance, with a goal of determining the implications for producing thick, highly contaminated komatiite flows. We adapted the model described above to investigate the results of eroding several endmember cases, including: 1) an anhydrous, consolidated tuff; 2) a hydrous, partly consolidated tuff; and 3) a hydrous, unconsolidated tuff. We ran our model for a variety of flow thicknesses (10m, 30m, 100m) and lava compositions (25-32% MgO) to determine how emplacement and erosion potential changes under these different initial conditions. We also assumed the lava was erupted at its liquidus temperature and at a pressure of 100 bars (i.e., under ~ 1 km of ocean). We assumed a relatively flat submarine slope (0.1º) and no topographic controls on emplacement. Because we have independent geochemical modeling data suggesting the Perseverance lavas were contaminated ~10-20%, we calculated the flow distance, thermal erosion rate, etc. for our model predictions within that range of contamination. We also constrained the model results to crustal thicknesses of ≤10 cm.

We first discuss the effect of the different substrates. For komatiite flow over an anhydrous, consolidated felsic tuff, we were unable to attain a degree of contamination in the lava ≥10% for flows emplaced at liquidus/subliquidus temperatures. However, if the lava was superheated ~200ºC above its liquidus temperature, then contamination of ~10-11% is obtained at a distance of >1000 km from the. Lava channels this large are not found on Earth, although some extraterrestrial lava channels have been found that are thousands of km long[4]. At these distances, even with superheating, model lava erosion rates are insufficient to produce ~100m deep channels for eruption durations of ~1 month.

For komatiite flow over a hydrous (50% H_2O), partly-consolidated (i.e., welded) felsic tuff, we report the results for both superheated (200ºC above liquidus) and non-superheated cases, assuming that only 10% of the heat of fusion of the substrate is required to unweld the tuff[5]. For non-superheated flows, contamination of ~10% corresponds once again to a flow distances >1000 km and to low erosion rates (~0.6 m/day). Such erosion rate requires an eruption duration to remove 100m of welded tuff of ~170 days (5.7 months). The estimated flow rate under these model eruption conditions is ~2.1 x 10^5 m^3/s (8.2 m/s x 25m thick x 1000m wide) which, for the eruption duration given above, indicate that the total flow volume would be ~3.0 x 10^3 km^3, about 2 orders of magnitude less than the entire Columbia River flood basalt province (CRB volume = 1.7 x 10^5 km^3: Tolan et al., 1989). Although there are one or two

[4] For example, Hildr Fossa on Venus is a long, canali-type lava channel that is continuous for over 6800 km in length (Head et al., 1991). The composition and emplacement conditions required to produce this channel are unknown.

[5] This parameter is unknown, but has been estimated assuming that the tuff crystals were anhedral, moderately well-sorted, and loosely-packed.

flows in the CRBs approaching this volume (Tolan et al., 1989), these flow distances, eruption durations, and flow volumes also seem unlikely. In contrast, for superheated lavas, contamination of ~10-16% corresponds to flow distances of a few hundred km and higher erosion rates (~7-3 m/day). These erosion rates require eruption durations to remove 100m of welded tuff of ~17-33 days. For the same flow rate given above and these eruption durations, total flow volumes are ~300-590 km^3, in the range of the average volume per flow of CRB flow units (Tolan et al., 1989). These flow distances, eruption durations, and flow volumes seem more likely.

For our final case, komatiite flow over a hydrous (50% H_2O), unconsolidated felsic tuff, we report results for non-superheated flows of a variety of initial thicknesses (Fig. 8). For an initially 10m thick komatiite flow, the model results indicate that high degrees of contamination (~10-20%) are obtained at distances of ~20-100 km from the eruption source for flows with very high erosion rates (~15-4.4 m/day). For an initially 30m thick komatiite flow, high degrees of contamination (~10-20%) are obtained at distances of ~100-440 km from the eruption source for flows with higher erosion rates (~20-5.9 m/day), and for an initially 100m thick komatiite flow, high degrees of contamination (~10-20%) are obtained at distances of ~450-1950 km from the eruption source for flows with still higher erosion rates (~30-9.5 m/day). In all cases, the vaporization of intergranular sea water fluidizes particles with sizes < very fine sand (i.e., particle diameters < 0.125 mm), thus generating high thermo-mechanical erosion rates and high degrees of contamination. Although the phenocrysts of the felsic tuff are course-sand sized (S.J. Barnes, pers. comm., 1997), the groundmass particle size is unknown and we assume that a finer-grained groundmass could have been fluidized by vaporized intergranular sea water, making it easier to remove the remaining material by mechanical erosion. At the erosion rates consistent with the distances given above, only relatively short eruption durations (~6.7-23 days for an initially 10m thick flow, ~5-17 days for an initially 30m thick flow, and ~3.3-11 days for an initially 100m thick flow) are required to remove 100m of unconsolidated tuff. For the latter case, a high flow rate, rapidly emplaced, highly erosive eruption would be consistent with the "cataclysmic" komatiite flood-like eruptions originally proposed by Barnes et al. (1988) and Hill et al. (1990,1995). If the lavas were superheated, then high degrees of contamination (10-20%) occur closer to the source (10s to <1000 km downstream) due to extended emplacement at higher erosion rates.

The key results of the modeling may be summarized as follows:

1) It is easier to erode a hydrous, unconsolidated tuff than a hydrous, partly consolidated, welded tuff than an anhydrous, massive tuff.

2) A thick (>10m), non-superheated, 32% MgO Perseverance flow(s) that is thermally and/or mechanically eroding a tuffaceous submarine substrate must travel hundreds to thousands of km to attain the level of contamination (~10-20%) predicted by the geochemical modeling of S.J. Barnes.

3) If the Perseverance lava was superheated ~200º above its liquidus, this higher temperature lava could have produced greater degrees of contamination at distances much closer to the source. For example, our modeling suggests that an initially 100m thick, superheated, 32% MgO komatiite flow would have produced high degrees of contamination (~10-20%) at distances of ~525-925 km from the eruption. At the erosion rates consistent with this distance (~64-51 m/day), a relatively short eruption duration (<2 days) is required to remove 100m of unconsolidated tuff. These values imply a flow volume of ~350 km^3, consistent with a short, cataclysmic eruption (Barnes et al., 1988; Hill et al., 1990). The likelihood of such a scenario is, however, debatable.

4) If the dacitic tuff substrate at Perseverance was hydrous, unconsolidated, and dominated by particles with sizes less than very fine sand (≤0.125 mm), then komatiite emplacement and erosion as envisioned by Barnes et al. (1988) was physically possible, and our modeling results seem plausible. For an initially 100m thick flow, an embayment ~100m deep could have been produced by thermo-mechanical erosion within a few hundred kilometers of the source quite quickly (~11 days), and for a flow rate ~2.1 x 10^6 m^3/s, this eruption duration corresponds to flow volumes <2000 km^3, which is about three times the average flow volume of CRB flows (Tolan et al., 1989). In this case, superheating is not required to produce a large degree of lava contamination (≤10%).

5) If the Perseverance tuff was hydrous and partly consolidated (i.e., a less erodable welded tuff), then superheating is required to give the Perseverance lavas the ability to erode this substrate within geologically reasonable flow distances (<1000 km downstream).

For example, if the lavas were superheated (e.g., 200ºC above liquidus), and if only a fraction of the latent heat (10%) is required to melt a partly consolidated, water-rich welded tuff, then high degrees of lava contamination (10-16%) can be attained within several hundred km of the source, and a deep, (~100 m) Perseverance-type embayment can be formed in a few weeks to a month.

6) Because most welded tuffs have only a fraction of their volume welded, with most of the remaining material unconsolidated, the nature of komatiite emplacement at Perseverance likely falls somewhere between 4) and 5) above. Thus, at a minimum, the style of lava emplacement at Perseverance probably included lava flow(s) that a) had traveled a few hundred km (in order to produce a contamination of ~10-20%), and that b) had volumes of a few hundred km^3 (in order to produce erosion of a deep (~100 m) embayment).

Katinniq

The Cape Smith Belt is a mid-Proterozoic (~1.8-1.9 Ga) volcano-sedimentary fold and thrust belt located on the Ungava peninsula of northern Québec (St-Onge and Lucas, 1993). In the east-central part of the belt, the Proterozoic Chukotat Group contains several komatiitic peridotite exposures that are among the best preserved, least metamorphosed komatiitic lava channels on Earth (Gillies, 1993; Lesher and Thibert, in prep.). One of these exposures is the Katinniq Peridotite Complex (KPC), which is a large lens-shaped outcrop (2.3 km long, 150-300m wide) consisting of at least 9 overlapping komatiitic peridotite flow units, each of which is ~10m thick with crustal (massive basalt or basaltic flow-top breccia) thicknesses of ~1-2m (Gillies, 1993). The KPC (Fig. 9) occupies a broad, ~100m deep concave embayment with smaller, second-order reentrants, which has been interpreted as a thermal erosion channel (Gillies, 1993; Lesher and Charland, in prep.). Geochemical analyses of the KPC show variations that are consistent with fractionation and accumulation of olivine ± chromite from an original komatiitic basalt lava with ~18% MgO (Barnes et al., 1982; Gillies, 1993; Burnham et al., in prep.).

The substrate underlying Katinniq is a laterally extensive (>10 km strike length), coarse-grained, differentiated gabbroic sheet flow (e.g., Lesher and Charland, in prep.). It has a maximum true thickness of ~100m and can be subdivided into several discrete zones, including (from base to top) a partially-exposed pyroxenitic zone, a thick mesogabbroic zone, a thin melanogabbroic zone, a thin leuco- to ferrogabbroic zone, and a thin (~1m) basaltic upper chilled margin (Lesher and Charland, in prep.), overlain by a ~10m thick interflow sedimentary horizon. Each of these zones is progressively transgressed by the KPC. It is possible that zones which contain slightly higher proportions of lower melting temperature minerals (e.g., quartz, plagioclase, and possibly amphibole) may partially melt at slightly lower temperatures, thus making some zones of the gabbro more thermally erodable than others, although all zones appear to have been eroded in the central part of the embayment. It is also possible that the gabbro may have been warm when it was eroded, but the fine-grained nature of the sediments suggests that they accumulated slowly and that the gabbro would have had time to cool completely.

The presence of a broad, concave embayment with smaller, second-order reentrants that is filled with multiple, overlapping thinner flow units (Fig. 9) suggests multi-stage lava emplacement (Lesher and Charland, in prep.). For example, the broad concave shape of the large first-order embayment requires that the embayment was once completely filled with lava, implying an initial flow thickness of ~100 m. However, the reentrant shape of the small second-order embayments on the floor of the larger channel, suggests either subchannelization and enhanced thermal erosion by basal sulphide-rich lavas and/or partial drainage and refilling. The presence of multiple, thin (ave. 10 m) flows in the main channel is consistent with drainage and refilling. Thus, we have modeled the emplacement of the ~10m thick flows that presently occupy the embayment, as well as the emplacement of the ~100m flow that may have produced the large, concave embayment, assuming that they were of similar composition and came from the same source. The ~1-2m thick flow-top breccias overlying the komatiitic peridotite flows are interpreted to be crusts (similar to fragmental crusts on modern, fast-moving, channelized ‘a’a basalt flows).

The precise degree of contamination at Katinniq is difficult to calculate, as contamination is more pronounced in the cumulate rocks than in the basaltic rocks, but work in progress suggests that it is of the order of 10% and that it appears to reflect a felsic rather than mafic contaminant (Burnham et al., in press). This apparent discrepancy can be explained by assuming that the contaminant preserved in the lavas

that have filled the channel is graphitic, sulphidic, semi-pelitic sediment that was exposed beneath the gabbro "upstream" from the present location, analogous in the reverse sense to the exposure of basalt beneath sulphidic sediments at Kambalda (see discussion by Lesher and Stone, 1996). Nevertheless, as most of the erosion was through gabbro, we have modeled thermal erosion of gabbro.

Because we are not certain whether the medium- to coarse-grained gabbroic substrate at Katinniq may have been more erodable than finer-grained basaltic substrates or whether it was completely cool prior to emplacement of the komatiitic basalt flows, we have run our model for three cases: 1) emplacement over a gabbroic substrate at T_{mg} = 1060ºC and T_a = 0ºC (i.e., assuming that the gabbro had thermal characteristics similar to basalt); 2) emplacement over a gabbroic substrate at T_{mg} = 960ºC and T_a = 0ºC (i.e., assuming a ~100ºC lower melting temperature for gabbro compared to basalt); and 3) emplacement over a gabbroic substrate at T_{mg} = 1060ºC and T_a = 600ºC (assuming the gabbro was still warm).

Case 1: The model for 10m thick flows predicts crustal thickness equivalent to the field measurements (flow-top breccias ~1-2m thick) at emplacement distances of ~160-250 km from the eruption source (Fig. 10a). Over this range of distances, the model results predict that a 100m thick flow would be a fast (~10-17 m/s) and turbulent (Re >10^6) with erosion rates ~0.8-0.7 m/day. To erode 100m of a consolidated gabbroic substrate would require eruption durations of ~125-143 days (~4-5 months) and the lava would have been negligibly contaminated (<0.1%). The 10m thick flows currently occupying the embayment are predicted to be contaminated ~1-2%, which would be difficult to resolve geochemically or isotopically.

Case 2: The model for 10m thick flows predicts crustal thickness equivalent to the field measurements at emplacement distances of ~120-180 km from the eruption source (Fig. 10b). Over this range of distances, the model results predict that a 100m thick flow would have higher erosion rates over the lower melting temperature substrate, ~1.1 m/day. To erode 100m of gabbroic substrate would require shorter eruption durations, ~90 days (~3 months), and this flow would also have been negligibly contaminated (<0.1%). In this model, the 10m thick flows currently occupying the embayment are also predicted to be contaminated ~1-2%.

Case 3: The model for 10m thick flows predicts crustal thickness equivalent to the field measurements at emplacement distances of ~140-220 km from the eruption source (Fig. 10c). Over this range of distances, the model results predict that a 100m thick flow would have higher erosion rates over the warmer substrate, ~1.4-1.3 m/day. To erode 100m of gabbroic substrate would require eruption durations of ~70-77 days (~2.5 months), and this flow would have only slightly higher contamination, ~0.1-0.2%. In this model, the 10m thick flows currently occupying the embayment are also predicted to have slightly higher contamination, ~2-2.5%.

The key results of the modeling may be summarized as follows:

1) As expected, it is easier to erode a warm gabbro than a cold gabbro, and it is easier to erode a gabbro than a basalt of the same composition, if the gabbro melts at a eutectic temperature lower than the solidus temperature of the basalt.

2) The amount of contamination resulting from thermal erosion of gabbro by komatiitic basalt is negligible, indicating that the observed contamination at Katinniq must be attributable to thermal erosion of sediment during the late stages of emplacement.

3) The rate of thermal erosion by a 100m thick flow is much greater than for a 10m thick flow, and it remains higher for a greater time and distance. If the gabbro was not warm and if it did not melt at a lower temperature than a basalt, it seems necessary that the deep channel at Katinniq formed from a thick flow at high flow rates.

DISCUSSION

Discussion of Model Results

The results of our lava emplacement and thermal erosion models suggest that although there is a great deal of uncertainty in modeling due to the very limited nature of model-constraining field data (e.g., flow thickness, embayment shape and depth, nature of the substrate) and some thermal/rheological/fluid dynamic parameters, the physics of komatiitic lava emplacement clearly support the potential for thermal/mechanical erosion of substrates at Kambalda, Perseverance, and Katinniq. In general, the potential for thermal/mechanical erosion increases as the lava becomes more magnesian (and therefore hotter) and/or superheated, and as the substrate

becomes more water-rich, more fragmental, and/or finer-grained. Large-scale (10s of meters) thermal erosion appears restricted to large lava channels (e.g., Perseverance, Katinniq), whereas small-scale (<10 m) thermal erosion occurs in channelized sheet flows (e.g., Kambalda). At Kambalda, both the field/geochemical evidence and the modeling support the hypothesis that sulphide-rich sediments were eroded and assimilated by the komatiite lava. If the komatiite flows at Perseverance are contaminated ~10-20% (S.J. Barnes, pers. comm., 1997) and were emplaced as thick (tens of meters) flows, then our modeling suggests large-scale thermo/mechanical erosion of the tuffaceous substrate may have been possible, especially if the tuffaceous substrate was unconsolidated and became fluidized and/or the komatiite was superheated.

At Katinniq, where cooler, less magnesian komatiitic basalt flows were emplaced over a more massive, consolidated gabbroic substrate, larger flow rates ($>10^3$ m^2/s) and/or longer eruptions (~months) would be required to produce such a large embayment by thermal erosion. If the melting temperature of the gabbro substrate was lower than basaltic substrates (e.g., due to the presence of hydrous phases), then our modeling suggests slightly higher erosion rates can occur, and thus shorter eruption durations are required to produce a deep embayment like Katinniq. Alternatively, a warmer gabbroic substrate is also easier to erode, although at Katinniq the layer of sediments above the gabbro indicates a significant volcanic hiatus between the emplacement of the gabbro and the komatiitic flows, and thus the gabbro was likely to have cooled. Also, partial melting followed by mechanical erosion (which should have played some role due to the very turbulent nature of the thick lava flow) may have aided in the formation of a deep embayment. Nevertheless, whether these other factors were present or not, our work suggests that high flow rates (i.e., very focused, turbulent flow) are required to produce an embayment like Katinniq.

Applications to the Genesis of Fe-Ni-Cu-(PGE) Sulphide Deposits

Most models for the genesis of magmatic Fe-Ni-Cu-(PGE) sulphide (see reviews by Naldrett, 1989; Lesher, 1989; Lesher and Stone, 1996) involve incorporation of crustal sulphur by devolatilization (e.g., Ripley, 1986; Poulson and Ohmoto, 1989), incongruent melting (Lesher et al., 1999), or wholesale melting (Groves et al., 1986; Lesher and Campbell, 1993) of sulphur-bearing country rocks. The results of our modeling (and previous workers) therefore have several important implications for the genesis of these deposits:

1) The erodability of different substrates may vary by an order of magnitude or more, depending on texture, composition, water content, and degree of consolidation. Phaneritic rocks (e.g., gabbro) may be more erodable than aphanitic rocks (e.g., basalt). Water-saturated unconsolidated rocks (e.g., sediments, unwelded tuffs, volcanic breccias) are more erodable than consolidated/welded rocks.

2) Although laminarly-flowing lavas are capable of thermal erosion (e.g., Kauahikaua et al., 1998), especially if they are high temperature lavas with sustained flow (weeks to months), turbulently-flowing lavas appear to be much more efficient in transferring heat from the lava to the country rocks. Thus, confined turbulent flows (lava channels and magma conduits) that maximize thermal erosion may be the most prospective areas to form magmatic ore deposits.

3) Higher temperature/lower viscosity magmas (e.g., komatiites and komatiitic basalts) will flow turbulently at lower flow rates than lower temperature/higher viscosity magmas (e.g., picrites and basalts), but all basic and ultrabasic magmas are capable of turbulent flow at sufficiently high (but geologically reasonable) flow rates.

4) Because lower-viscosity fluids are more likely to become channelized than higher viscosity fluids (e.g., komatiite lavas vs. basaltic lavas), magmatic Fe-Ni-Cu-(PGE) deposits are more likely to form in komatiite lavas than in basaltic lavas. Furthermore, because komatiitic basaltic and basaltic magmas must flow at higher rates than komatiites to maintain turbulent flow, the host units in komatiitic basaltic and basaltic systems must be larger than those in komatiitic systems.

5) With all other parameters equal (discharge rate, lava thermal properties, substrate thermal properties), lava channels and tubes, in which lava flow is confined and focussed by levees and/or topography, are capable of greater degrees of thermal erosion than sheet flows, in which flow is less focussed (Fig. 11: see also Jarvis, 1995).

6) The cumulate rocks that are commonly used to define and recognize lava channels and magma

conduits formed after the thermal-erosional stage. As lava channels or magma conduits may pond or drain and refill after the ore-forming thermal-erosional stage, it is possible to produce a differentiated unit that in many respects (mineralogy, texture, and composition) is similar or identical to a unit that formed in an unchannelized system. However, most of the thermal erosion channels that have been identified are filled with cumulate rocks indicating that they normally continued flowing for a relatively long time before ponding.

7) The rate of thermal erosion (and hence the rate of sulphide melting) is a function of heat transfer (which depends upon Reynolds number, and hence flow rate, to the power 0.8). Thus, for a fixed volume of lava, a system with a lower flow rate that flows for a longer period of time may form a larger ore deposit than a system that flows at a higher flow rate for a shorter period of time. Sulphides may not accumulate near the site of thermal erosion, but may be transported significant distances depending on the geometry of the plumbing system and the fluid dynamics. In some places (e.g., Kambalda) sulphide ores are overlain by barren, uncontaminated host rocks (Lesher and Arndt, 1995). This indicates that the S-bearing contaminant was exhausted upstream and/or that the fluid dynamic regime changed with time, and that the lava channel was replenished with uncontaminated, sulphide-undersaturated lava (Lesher and Stone, 1996). It also implies that the flow rate declined to a level where it was not capable of re-eroding the sulphides, although this is a likely explanation for the massive/net-textured/disseminated ore segregation profile in many dynamic ore-forming systems.

8) With all other parameters equal (dimensions, flow rate, thermal properties), an intrusive magma conduit will lose heat more slowly than an extrusive lava channel and will therefore have a greater potential for thermal erosion. This may be mitigated by the fact that lava channels are often erupted onto S-rich substrates, whereas a channelized sills are less often intruded along sulphur-rich country rocks. Nevertheless, many of the world's largest deposits of this type (e.g., Noril'sk, Jinchuan, Voisey's Bay) are intrusive.

9) Although not addressed specifically in this study, field, geochemical, and isotopic studies indicate that sulphur may be devolatilized from S-rich sediments before they melt (Ripley, 1986; Poulson and Ohmoto, 1989; Lesher and Thibert, in prep.) and that some sediments may partially melt (Lesher et al., 1999). Thus, wholesale assimilation is not essential to the formation of an ore deposit and the temperatures and conditions required for ore genesis may be wider than those for thermal-mechanical erosion.

OUTSTANDING QUESTIONS AND PROBLEMS

In terms of understanding the dynamics of magmatic ore-forming systems, the mathematical modeling described here is useful for investigating the first part of the problem regarding komatiite-hosted magmatic sulphides; i.e., how hot, fluid, turbulent komatiites can thermally erode and assimilate sulphide-rich materials and evolve the composition of the lava. The other part of the problem involves the investigation of the thermodynamics of the metal sulphide liquids and the physics of segregation of the sulphide melts from the komatiite lavas. This problem has yet to be rigorously addressed. Further study is also required to better understand the relationships between komatiitic lava crusts and style of emplacement, between olivine crystallization and resulting changes in flow regime, and between substrate composition and morphology and erosive potential by komatiitic lavas.

SUMMARY

We have reviewed the thermal and fluid dynamics of Archean and Proterozoic komatiitic lavas. Compared to modern basaltic lavas, komatiitic lavas are thought to have had lower SiO_2 and higher MgO contents, resulting in higher liquidus and (potentially) eruption temperatures, higher heat contents, lower dynamic viscosities, and lower thermal conductivities. Consequently, komatiitic lavas are thought: (1) to have been very fluid and emplaced as turbulent flows; (2) to have lost heat primarily through convective transfer to the surroundings; (3) to have produced flows that could have attained great areal extents through the insulating effects of surficial crusts; and (4) to have had a great potential to thermally erode their underlying substrates and to contaminate themselves with assimilated substrate melt. Thermally-eroding komatiitic lavas have been proposed as the source of embayments that contain komatiite-hosted magmatic sulphide deposits, and the cumulate rocks that fill the embayments are thought to be the remnants of large lava channels. We have developed a mathematical computer model to simulate the thermal, rheological, fluid dynamic, and geochemical evolution of komatiitic lava flows during emplacement, based on assumptions of initial

eruption temperature, flow thickness, ground slope, and lava and substrate composition, and we have applied this model to investigate the nature of komatiite emplacement at Kambalda and Perseverance in the Norseman-Wiluna greenstone belt of Western Australia and Katinniq in the Cape Smith belt of New Québec, Canada. Our model results for Kambalda support the interpretation based on field/geochemical evidence that komatiite lavas eroded sulphide-rich sediment that may have led to the formation of magmatic sulphide liquids that settled at the base of lava channels. Our model results for Perseverance suggest that large-scale thermal erosion and contamination of thick komatiite flows could have occurred if the lavas were superheated and/or the tuffaceous substrate was water-rich and either unconsolidated or loosely welded. Our model results for Katinniq indicate either that larger and/or longer eruptions of cooler, lower MgO komatiitic basalt lava are required to form a large embayment in a massive, consolidated gabbroic substrate. Nevertheless, the presence of massive sulphides at all three of these localities where thermal erosion has been inferred indicate the potential importance of the link between komatiitic lava emplacement, thermal erosion, and the formation of komatiite-hosted magmatic sulphide deposits. Further work should concentrate on understanding the thermodynamic and geochemical changes required to produce sulphide liquids from contaminated komatiitic lavas, the processes that lead to sulphide segregation, and the effects on komatiite heat loss when massive sulphide deposits accumulate at the base of the flows.

ACKNOWLEDGMENTS

This work stems from the doctoral research of D.A.W., which was supported primarily by University of Alabama Graduate Council Research Fellowships and secondarily by the National Science Foundation (EAR-9405994). Field work in the Cape Smith, Abitibi, and Norseman-Wiluna greenstone belts was generously supported by Falconbridge Ltd., Outokumpu Ltd., and WMC Resources Ltd., respectively. Geochemical studies at Perseverance, Kambalda, and the Cape Smith Belt were supported by WMC Resources Ltd. and the National Science Foundation (EAR-8820126 and EAR-9018938). R.C.K. was supported by an Australian Research Council Fellowship. We thank Steve Self for a very helpful review.

REFERENCES

Arndt, N.T., 1976, Melting relations of ultramafic lavas (komatiites) at one atmosphere and high pressure, Carnegie Institute Geophysical Laboratory Yearbook, v. 75, p. 555-562.

Arndt, N.T., and E.G. Nisbet, 1982, Komatiites, George Allen and Unwin, London, 526 pp.

Arndt, N.T., D.M. Francis, and A.J. Hynes, 1979, The field characteristics and petrology of Archean and Proterozoic komatiites, Canadian Mineralogist, v. 17, p. 147-163.

Arndt, N., C. Ginibre, C. Chauvel, F. Albarede, M. Cheadle, C. Herzberg, G. Jenner, Y. Lahaye, 1998, Were komatiites wet?, Geology, v. 26, p. 739-742.

Baird, A.K., 1984, Did komatiitic lavas erode channels on Mars?, Nature, v. 311, p. 18.

Baker, V.R., G. Komatsu, T.J. Parker, V.C. Gulick, J.S. Kargel, J.S. Lewis, 1992, Channels and valleys on Venus: Preliminary analysis of Magellan data, Journal of Geophysical Research, v. 97, p. 13,421-13,444.

Barnes, S.J., C.J.A. Coats, and A.J. Naldrett, 1982, Petrogenesis of a Proterozoic nickel sulfide-komatiite association: the Katiniq Sill, Ungava, Quebec, Economic Geology, v. 77, p. 413-429.

Barnes, S.J., R.E.T. Hill, and M.J. Gole, 1988, The Perseverance Ultramafic Complex, Western Australia: The product of a komatiite lava river, Journal of Petrology, v. 29, p. 302-331.

Barnes, S.J., C.M. Lesher, and R.R. Keays, 1995, Geochemistry of mineralized and barren komatiites from the Perseverance nickel deposit, Western Australia, Lithos, v. 34, p. 209-234.

Bavinton, O.A., 1981, The nature of sulfidic metasediments at Kambalda and their broad relationships with associated ultramafic rocks and nickel ores, Economic Geology, v. 76, p. 1606-1628.

Beattie, P., C. Ford, and D. Russell, 1991, Partition coefficients for olivine-melt and orthopyroxene-melt systems, Contributions to Mineralogy and Petrology, v. 109, p. 212-224.

Beattie, P., C. Ford, and D. Russell, 1993, Partition coefficients for olivine-melt and orthopyroxene-melt systems, Contributions to Mineralogy and Petrology, v. 114, p. 288.

Birch, F. and H. Clark, 1940, The thermal conductivity of rocks and its dependence upon temperature and composition, American Journal of Science, v. 238, p. 529-558 & 613-635.

Bottinga, Y., and D.F. Weill, 1970, Densities of liquid silicate systems calculated from partial molar volumes of oxide components, American Journal of Science, v. 269, p. 169-182.

Burnham, O.M., C.M. Lesher, and R.R. Keays, in preparation, Geochemistry and petrogenesis of komatiitic basalts, gabbros, and peridotites in the Cape Smith Belt, New Quebec, in Lesher, C.M., ed., Field Guide to Magmatic Fe-Ni-Cu-(PGE) Deposits in the Cape Smith Belt, New Quebec, Society of Economic Geologists, Guidebook Series.

Bussey, D.B.J., S.-A. Sørensen, and J.E. Guest, 1995, Factors influencing the capability of lava to erode its substrate: Application to Venus, Journal of Geophysical Research, v. 100, p. 16,941-16,948.

Carr, M.H., 1974, The role of lava erosion in the formation of lunar rilles and Martian channels, Icarus, v. 22, p. 1-23.

Coombs, C.R., B.R. Hawke, and L. Wilson, 1990, Terrestrial analogs to lunar sinuous rilles: Kauhako crater and channel, Kalaupapa, Molokai, and other Hawaiian lava conduit systems, Proceedings of 20th Lunar and Planetary Science Conference, p. 195-206.

Cowden, A., 1988, Emplacement of komatiite lava flows and associated nickel sulphides at Kambalda, Western Australia, Economic Geology, v. 83, p. 436-442.

Crisp, J., and S. Baloga, 1990, A model for lava flows with two thermal components, Journal of Geophysical Research, v. 95, p. 1255-1270.

Cruikshank, D.P., and C.A. Wood, 1972, Lunar rilles and Hawaiian volcanic features: Possible analogs, The Moon, v. 3, p. 412-447.

Cutts, J.A., W.J. Roberts, and K.R. Blasius, 1978, Martian channels formed by lava erosion (abstract), Lunar and Planetary Science IX, p. 209.

Dawson, J.B., H. Pinkerton, G.E. Norton, and D.M. Pyle, 1990, Physicochemical properties of alkali carbonatite lavas: Data from the 1988 eruption of Oldoinyo Lengai, Tanzania, Geology, v. 18, p. 260-263.

Evans, D.M., A. Cowden, and R.M. Barratt, 1989, Deformation and thermal erosion at the Foster nickel deposit, Kambalda-St. Ives, Western Australia, *in* Prendergast, M.D., and M.J. Jones, eds., Magmatic Sulphides – The Zimbabwe Volume, London, Institution of Mining and Metallurgy, p. 215-219.

Frost, K.M., and D.I. Groves, 1989, Ocellar units at Kambalda: Evidence for sediment assimilation by komatiite lavas, *in* Prendergast, M. D., and M. J. Jones, eds., Magmatic Sulphides – The Zimbabwe Volume, London, Institution of Mining and Metallurgy, p. 207-213.

Ghiorso, M.S., and R.O. Sack, 1995, Chemical mass transfer in magmatic processes IV. A revised and internally consistent thermodynamic model for the interpolation and extrapolation of liquid-solid equilibria in magmatic systems at elevated temperatures and pressures, Contributions to Mineralogy and Petrology, v. 119, p. 197-212.

Gillies, S.L., 1993, Physical volcanology of the Katinniq peridotite complex and associated Fe-Ni-Cu-(PGE) mineralization, Cape Smith Belt, New Quebec, Unpublished M.S. thesis, University of Alabama, Tuscaloosa, 146 pp.

Greeley, R., 1971a, Geology of selected lava tubes in the Bend Area, Oregon, State of Oregon Department of Geology and Mineral Resources Bulletin, v. 71, p. 1-47.

Greeley, R., 1971b, Observations of actively forming lava tubes and associated structures, Hawaii, Modern Geology, v. 2, p. 207-223.

Greeley, R., 1972, Additional observations of actively forming lava tubes and associated structures, Hawaii, Modern Geology, v. 3, p. 157-160.

Greeley, R., and J.H. Hyde, 1972, Lava tubes of the Cave Basalt, Mount St. Helens, Washington, *Geological Society of America Bulletin, v. 83*, p. 2397-2418.

Greeley, R., S.W. Lee, D.A. Crown, and N. Lancaster, 1990, Observations of industrial sulfur flows: Implications for Io, Icarus, v. 84, p. 374-402.

Greeley, R., S.A. Fagents, R.S. Harris, S.D. Kadel, D.A. Williams, and J.E. Guest, 1998, Evidence for erosion by flowing lava and planetary implications, Journal of Geophysical Research, v. 103, p. 27,325-27,346.

Gresham, J.J., and G.D. Loftus-Hills, 1981, The geology of the Kambalda nickel field, Western Australia, Economic Geology, v. 76, p. 1373-1416.

Groves, D.I., E.A. Korkiakoski, N.J. McNaughton, C.M. Lesher, and A. Cowden, 1986, Thermal erosion by komatiites at Kambalda, Western Australia and the genesis of nickel ores, Nature, v. 319, p. 136-139.

Head, J.W., and L. Wilson, 1981, Lunar sinuous rille formation by thermal erosion: Eruption conditions, rates and durations (abstract), Lunar and Planetary Science XII, p. 427-429.

Head, J.W., D.B. Campbell, C. Elachi, J.E. Guest, D.P. McKenzie, R.S. Saunders, G.G. Schaber, and G. Schubert, 1991, Venus volcanism: Initial analysis from Magellan data, Science, v. 252, p. 276-288.

Herzberg, C. and M.J. O'Hara, 1998, Phase equilibrium constraints on the origin of basalts, picrites, and komatiites, Earth Science Reviews, v. 44, p. 39-79.

Hill, R.E.T., S.J. Barnes, M.J. Gole, and S.E. Dowling, 1990, Physical volcanology of komatiites, Excursion Guidebook #1, Geological Society of Australia (Western Australia Division), Perth, 100 pp.

Hill, R.E.T., S.J. Barnes, M.J. Gole, and S.E. Dowling, 1995, The volcanology of komatiites as deduced from field relationships in the Norseman-Wiluna greenstone belt, Western Australia, Lithos, v. 34, p. 159-188.

Holman, J.P., 1986, Heat Transfer, 6th edition, McGraw-Hill, New York, 676 pp.

Hon, K., J. Kauahikaua, R. Delinger, and K. Mackay, 1994, Emplacement and inflation of pahoehoe sheet flows: Observations and measurements of active lava flows on Kilauea Volcano, Hawaii, Geological Society of America Bulletin, v. 106, p. 351-370.

Hulme, G., 1973, Turbulent lava flows and the formation of lunar sinuous rilles, Modern Geology, v. 4, p. 107-117.

Hulme, G., 1974, The interpretation of lava flow morphology, Geophysical Journal of the Royal Astronomical Society, v. 39, p. 361-383.

Hulme, G., 1982, A review of lava flow processes related to the formation of lunar sinuous rilles, Geophysical Surveys, v. 5, p. 245-279.

Huppert, H.E., and R.S.J. Sparks, 1985a, Komatiites I: Eruption and flow, Journal of Petrology, v. 26, p. 694-725.

Huppert, H.E., and R.S.J. Sparks, 1985b, Cooling and contamination of mafic and ultramafic magmas during ascent through continental crust, Earth & Planetary Science Letters, v. 74, p. 371-386.

Huppert, H.E., R.S.J. Sparks, J.S. Turner, and N.T. Arndt, 1984, Emplacement and cooling of komatiite lavas, Nature, v. 309, p. 19-22.

Jarvis, R.A. , 1995, On the cross-sectional geometry of thermal erosion channels formed by turbulent lava flows, Journal of Geophysical Research, v. 100, p. 10,127-10,140.

Kakaç, S., R.K. Shah, and W. Aung, 1987, Handbook of Single-Phase Convective Heat Transfer, John Wiley & Sons, New York.

Kauahikaua, J., K. Cashman, K. Hon, T. Mattox, C. Heliker, M. Mangan, and C. Thornber, 1998, Observations on basaltic lava streams in tubes from Kilauea volcano, island of Hawai'i, Journal of Geophysical Research, v. 103, p. 27,303-27,324.

Kennedy, A.K., G.E. Lofgren, and G.J. Wasserburg, 1993, An experimental study of trace element partitioning between olivine, orthopyroxene, and melt in chondrules: Equilibrium values and kinetic effects, Earth and Planetary Science Letters, v. 115, p. 177-195.

Keszthelyi, L., and S. Self, 1998, Some physical requirements for the emplacement of long basaltic lava flows, Journal of Geophysical Research, v. 103, p. 27,447-27,464.

Kokini, J.L., 1992, Rheological properties of foods, in Handbook of Food Engineering, Heldman, D.R. and D.B. Lund, eds., Marcel Dekker, inc., New York, p. 1-38.

Komatsu, G., and V.R. Baker, 1994, Meander properties of Venusian channels, Geology, v. 22, p. 67-70.

Komatsu, G., V.R. Baker, V.C. Gulick, and T.J. Parker, 1993, Venusian channels and valleys: Distribution and volcanological implications, Icarus, v. 102, p. 1-25.

Lange, R.A., and A. Navrotsky, 1992, Heat capacities of Fe_2O_3-bearing silicate liquids, Contributions to Mineralogy & Petrology, v. 110, p. 311-320.

Lesher, C.M., 1989, Komatiite-associated nickel sulfide deposits, *in* Ore deposits associated with magmas, Whitney, J.A., and Naldrett, A.J., eds., Reviews in Economic Geology, v. 4, p. 45-102.

Lesher, C.M., and D.I. Groves, 1986, Controls on the formation of komatiite-associated nickel-copper sulfide deposits, in Geology and Metallogeny of Copper Deposits, Friedrich, G.H., A.D. Genkin, A.J. Naldrett, J.D. Ridge, R.H. Sillitoe, and F.M. Vokes, eds., Springer-Verlag, Berlin, p. 43-62.

Lesher, C.M., and I.H. Campbell, 1993, Geochemical and fluid dynamic modeling of compositional variations in Archean komatiite-hosted nickel sulfide ores in Western Australia, Economic Geology, v. 88, p. 804-816.

Lesher, C.M., and N.T. Arndt, 1995, REE and Nd geochemistry, petrogenesis, and volcanic evolution of contaminated komatiites at Kambalda, Western Australia, Lithos, v. 34, p. 127-158.

Lesher, C.M., and W.E. Stone, 1996, Exploration geochemistry of komatiites, in Igneous Trace Element Geochemistry Applications for Massive Sulfide Exploration, Wyman, D.A., ed., GAC-MAC Short Course Notes, v. 12, p. 153-204.

Lesher, C.M., and A. Charland, in preparation, Geology of the Katinniq Peridotite Complex and associated Fe-Ni-Cu-(PGE) mineralzation, Cape Smith Belt, New Quebec, in Lesher, C.M., ed., Field Guide to Magmatic Fe-Ni-Cu-(PGE) Deposits in the Cape Smith Belt, New Quebec, Society of Economic Geologists, Guidebook Series.

Lesher, C.M., and F. Thibert, in preparation, Stratigraphy and physical volcanology of komatiitic peridotite lava channels, channelized sheet flows, and channelized sheet sills in the Cape Smith Belt, New Quebec, in Lesher, C.M., ed., Field Guide to Magmatic Fe-Ni-Cu-(PGE) Deposits in the Cape Smith Belt, New Quebec, Society of Economic Geologists, Guidebook Series.

Lesher, C.M., N.T. Arndt, and D.I. Groves, 1984, Genesis of komatiite-associated nickel sulphide deposits at Kambalda, Western Australia: A distal volcanic model, in Sulphide deposits in mafic and ultramafic rocks, Buchanan, D.L., and M.J. Jones, eds., Institute of Mining and Metallurgy, London, p. 70-80.

Lesher, C.M., J.P. Golightly, and R.R. Keays, 1999, Dynamic incongruent melting in magmatic sulphide deposits, Geological Association of Canada-Mineralogical Association of Canada Annual Meeting, Abstract Volume.

Lide, D.R., 1993, CRC Handbook of Chemistry and Physics, 74th Ed., CRC Press, Inc., Boca Raton, Florida.

Malin, M.C., 1980, Lengths of Hawaiian lava flows, Geology, v. 8, p. 306-308.

McMillan, M.L., 1977, Engine oil viscosity classifications: Past, present, and future, in The Relationship between Engine Oil Viscosity and Engine Performance, Stewart, R.M., and Selby, T.W., eds., Society of Automotive Engineers, Warrendale, Pennsylvania, p. 21-32.

McNaughton, N.J., K.M. Frost, and D.I. Groves, 1988, Ground melting and ocellar komatiites: a lead isotopic study at Kambalda, Western Australia, Geological Magazine, v. 125, p. 285-295.

Murase, T., and A.R. McBirney, 1970, Thermal conductivity of lunar and terrestrial igneous rocks in their melting range, Science, v. 170, p. 165-167.

Murase, T. and A.R. McBirney, 1973, Properties of some common igneous rocks and their melts at high temperatures, Geological Society of America Bulletin, v. 84, p. 3563-3592.

Naldrett, A. J., 1989, Magmatic Sulfide Deposits, New York, Oxford University Press, 186 pp.

Navrotsky, A. , 1995, Energetics of silicate melts, in Structure, Dynamics and Properties of Silicate Melts, Stebbins, J.F., P.F. McMillan, and D.B. Dingwell, eds., Reviews in Mineralogy, v. 32, p. 121-142.

Nichols, R.L., 1939, Viscosity of lava, Journal of Geology, v. 47, p. 290-302.

Nisbet, E.G., 1982, The tectonic setting and petrogenesis of komatiites, in Komatiites, Arndt, N.T., and E.G. Nisbet, eds., George Allen and Unwin, London, 526 pp.

Nisbet, E.G., M.J. Cheadle, N.T. Arndt, and M.J. Bickle, 1993, Constraining the potential temperature of the Archaean mantle: A review of the evidence from komatiites, Lithos, v. 30, p. 291-307.

Norton, G.E., and H. Pinkerton, 1992, The physical properties of carbonatite lavas: Implications for planetary volcanism (abstract), Lunar and Planetary Science Conference XXIII, p. 1001-1002.

Parman, S.W., J.C. Dann, T.L. Grove, and M.J. de Wit, 1997, Emplacement conditions of komatiite magmas from the 3.49 Ga Komati Formation, Barberton Greenstone Belt, South Africa, Earth & Planetary Science Letters, v. 150, p. 303-323.

Peterson, D.W., and D.A. Swanson, 1974, Observed formation of lava tubes during 1970-71 at Kilauea Volcano, Hawaii, Studies in Speleology, v. 2, p. 209-222.

Peterson, D.W., R.T. Holcomb, R.I. Tilling, and R.L. Christiansen, 1994, Development of lava tubes in the light of observations at Mauna Ulu, Kilauea Volcano, Hawaii, Bulletin of Volcanology, v. 56, p. 343-360.

Poulson, S.R., and H. Ohmoto, 1989, Devolatilization equilibria in graphite-pyrite-pyrrhotite bearing pelites with application to magma pelite interaction, Contributions to Mineralogy and Petrology, v. 101, p. 418-425.

Ripley, E.M., 1986, Application of stable isotopic studies to problems of magmatic sulfide ore genesis with special reference to the Duluth complex, in: Friedrich, G.H., A.D. Genkin, A.J. Naldrett, J.D. Ridge, R.H. Sillitoe, and F.M. Vokes (eds.), Geology and Metallogeny of Copper Deposits, Springer-Verlag, Berlin, p. 25-42.

Ross, J.R., and G.A. Travis, 1981, The nickel sulfide deposits of Western Australia in global perspective, Economic Geology, v. 76, p. 1291-1329.

Ryan, M.P., and C.G. Sammis, 1981, The glass transition in basalt, Journal of Geophysical Research, v. 86, p. 9,516-9,539.

Self, S., T. Thordarson, L. Keszthelyi, G.P.L. Walker, K. Hon, M.T. Murphy, P. Long, and S. Finnemore, 1996, A new model for the emplacement of Columbia River basalts as large, inflated pahoehoe lava flow fields, Geophysical Research Letters, v. 23, p. 2689-2692.

Self, S., T. Thordarson, and L. Keszthelyi, 1997, Emplacement of continental flood basalt lava flows, in AGU Monograph on Large Igneous Provinces, Mahoney, J.J. and M. Coffin, eds., American Geophysical Union, p. 381-410.

Shaw, H.R., 1969, Rheology of basalt in the melting range, Journal of Petrology, v. 10, p. 510-535.

Shaw, H.R., 1972, Viscosities of magmatic silicate liquids: An empirical method of prediction, American Journal of Science, v. 272, p. 870-893.

Shaw, H.R., and D.A. Swanson, 1970, Eruption and flow rates of flood basalts, in Proceedings of the 2nd Columbia River Basalt Symposium, Gilmour, E.H. and D. Stradling, eds., Cheney, Eastern Washington State College Press, p. 271-299.

Snyder, D., E. Gier, and I. Carmichael, 1994, Experimental determination of the thermal conductivity of molten $CaMgSi_2O_6$ and the transport of heat through magmas, Journal of Geophysical Research, v. 99, p. 15,503-15,516.

Sparks, R.S.J., H. Sigurdsson, and S.N. Carey, 1980, The entrance of pyroclastic flows into the sea, II. Theoretical considerations on subaqueous emplacement and welding, Journal of Volcanology and Geothermal Research, v. 7, p. 97-105.

St-Onge, M.R., and S.B. Lucas, 1993, Geology of the eastern Cape Smith Belt; part of the Kangiqsujuac, Cratére du Nouveau-Québec, and lacs Nuvilik map areas, Québec, Geological Survey of Canada, Memoir 438, 110 pp.

Stebbins, J.F., I.S.E. Carmichael, and D.F. Weill, 1983, The high temperature liquid and glass heat contents and the heats of fusion of diopside, albite, sanidine and nepheline, American Mineralogist, v. 68, p. 717-730.

Stone, W.E., E. Deloule, M.S. Larson, and C.M. Lesher, 1997, Evidence for hydrous high-MgO melts in the Precambrian, Geology, v. 25, p. 143-146.

Swanson, D.A., 1973, Pahoehoe flows from the 1969-1971 Mauna Ulu eruption, Kilauea Volcano, Hawaii, Geological Society of America Bulletin, v. 84, p. 615-626.

Tolan, T., S.P. Reidel, M.H. Beeson, J.L. Anderson, K.R. Fecht, and D.A. Swanson, 1989, Revisions to the estimates of the areal extent and volume of the Columbia River Basalt Group, in Volcanism and Tectonism in the Columbia River Flood-Basalt Province, Reidel, S.P., and P.R. Hooper, eds., Geological Society of America Special Paper 239, p. 1-20.

Turcotte, D.L., and G. Schubert, 1982, Geodynamics, John Wiley, New York, 450 pp.

Usselman, T.M., D.S. Hodge, A.J. Naldrett, and I.H. Campbell, 1979, Physical constraints on the characteristics of nickel-sulfide ore in ultramafic lavas, Canadian Mineralogist, v. 17, p. 361-372.

Viswanath, D.S., and G. Natarajan, 1989, Data Book on the Viscosity of Liquids, Hemisphere Publishers, New York, 990 pp.

Walker, D., R.J. Kirkpatrick, J. Longhi, and J.F. Hays, 1976, Crystallization history of lunar picritic basalt sample 12002: Phase-equilibria and cooling-rate studies, Geological Society of America Bulletin, v. 87, p. 646-656.

Walker, G.P.L., 1973, Lengths of lava flows, Philosophical Transactions of the Royal Society of London, v. A274, p. 107-118.

Walker, G.P.L., 1991, Structure, and origin by injection of lava under surface crust, of tumuli, "lava rises", "lava-rise pits", and "lava-inflation clefts" in Hawaii, Bulletin of Volcanology, v. 53, p. 546-558.

Williams, D.A., 1998, Analytical/numerical modeling of the emplacement and erosional potential of Archean and Proterozoic komatiitic lavas, Unpublished Ph.D. dissertation, University of Alabama, 286 pp.

Williams, D.A., R.C. Kerr, and C.M. Lesher, 1998, Emplacement and erosion by Archean komatiite lava flows at Kambalda: Revisited, Journal of Geophysical Research, v. 103, p. 27,533-27,549.

Williams, H., and A.R. McBirney, 1979, Volcanology, Freeman, Cooper & Company, San Francisco, California, 397 pp.

Wilson, L., and P. Mouginis-Mark, 1984, Martian sinuous rilles (abstract), Lunar and Planetary Science XV, p. 926-927.

Wood, C., 1981, Exploration and geology of some lava tube caves on the Hawaiian volcanoes, Transactions of the British Cave Research Association, v. 8, p. 111-129.

FIGURE CAPTIONS

Figure 1. Graph of lava liquid dynamic viscosity vs. temperature for several mafic and ultramafic lava types. Komatiitic lavas have viscosities one- to two- orders of magnitude lower than modern basaltic lavas, suggesting they may have been capable of producing more areally-extensive flows than modern lavas.

Figure 2. Thermal conductivity data (top) and curve fit to best data (bottom) for high temperature, low viscosity silicate liquids. These data suggest that komatiitic liquids may have had an order of magnitude or more lower thermal conductivity than modern lavas. This lower conductivity would have resulted in reduced heat loss from turbulent flows if insulating crusts were formed.

Figure 3. Schematic diagram of a hypothetical, thermally-eroding submarine komatiite lava flow. Turbulent flow causes convective heat transfer to a growing surface crust and to a thermally eroding substrate if lava temperature T is greater than substrate melting temperature T_{mg}.

Figure 4. Graph of lava Reynolds number vs. lava flow thickness for several lava compositions. With the exception of carbonatite flows, modern lavas are restricted to the laminar flow regime for

most flow thicknesses (flow rates). In contrast, high temperature, low viscosity, Archean and Proterozoic komatiitic lava flows could have erupted in the turbulent regime even for very thin (<1 m) flows.

Figure 5. Schematic diagram of the ore environment at Kambalda, Western Australia (adapted from Lesher et al., 1984 and Groves et al., 1986). Ores are localized in flat-floored reentrant embayments in footwall basalts, the floors of which commonly correlate with flow unit boundaries in the adjacent basalt sequence (Lesher, 1989) and the margins of which are bordered by aphyric komatiites. Basal contacts grade laterally from ore-bearing through barren contact and chloritized sediment to unaltered sediment (Bavinton, 1981). Ores also occur at the bases of overlying flows, some of which have thermally-eroded the spinifex-textured zones of underlying flows, forming spinifex-textured ores and silicate domes (Groves et al., 1986).

Figure 6. Model results for the emplacement of an initially 10 m thick, 32% MgO Kambalda komatiite lava flow over consolidated sediment and basalt substrates and unconsolidated sediment substrate with slope of 0.1º.

Figure 7. Geologic map of the Perseverance Ultramafic Complex (after Barnes et al., 1988). Although the NW margin has been strongly modified by folding, the Perseverance Ultramafic Complex is interpreted to have thermally-eroded underlying felsic volcanic and volcaniclastic rocks, forming a broad, concave embayment.

Figure 8. Model results for the emplacement of initially 10m, 30m, and 100m thick, 32% MgO Perseverance komatiite lava flow over unconsolidated, hydrous felsic tuff substrate with slope of 0.1º.

Figure 9. Geologic map of the Katinniq Peridotite Complex, Cape Smith Belt, New Québec (mapping by C.M.L.). Komatiitic peridotites and pyroxenites occupy a broad, concave embayment that is interpreted to have formed by thermal erosion of underlying gabbroic and sedimentary substrates by komatiitic basalt lavas. Overlying basalts and sediments are not hornfelsed, but underlying and adjacent basalts, sediments, and gabbros are hornfelsed.

Figure 10a. Model results for the emplacement of 18% MgO Katinniq komatiitic peridotite lava flows over gabbroic substrate with slope of 0.1º. Ground melting temperature is 1060ºC, ambient temperature is 0ºC.

Figure 10b. Model results for the emplacement of 18% MgO Katinniq komatiitic peridotite lava flows over gabbroic substrate with slope of 0.1º. Ground melting temperature is 960ºC, ambient temperature is 0ºC.

Figure 10c. Model results for the emplacement of 18% MgO Katinniq komatiitic peridotite lava flows over gabbroic substrate with slope of 0.1º. Ground melting temperature is 1060ºC, ambient temperature is 600ºC.

Figure 11. Schematic diagram for the formation of thermal erosion lava channels and sulphide ore deposits during the emplacement of komatiitic lava flows (adapted from Lesher et al., 1984; Lesher, 1989; Hill et al., 1995). Topographic irregularities and declining temperatures in sheet flow facies promote channelization of lava, which concentrates heat and momentum in the channel. Thermal erosion and melting of S-rich substrates generates sulphide melts, which are denser and lower viscosity than the komatiitic lava and therefore accumulate at the base of the lava channels. Concave embayments are interpreted to form beneath flows overlying erodable substrates which have thicknesses above the eroded channel depth and/or which contain few sulphides. Reentrant channels are interpreted to form beneath flows overlying erodable substrates which have

thicknesses below the eroded channel depth (see Jarvis, 1995) and/or which contain basal layers of dense, low-viscosity sulphides (Groves et al., 1986; Lesher, 1989).

Table 1. Inferred original liquid compositions and their corresponding thermal/rheological properties for several komatiite localities in Archean and Proterozoic terrains.

Component/ Parameter	Archean Kambalda Komatiite	Archean Perseverance Komatiite	Proterozoic Komatiitic Basalt	Low-TiO_2 Lunar Mare Basalt	Tholeiitic Continental Flood Basalt
SiO_2	45.0	43.9	46.9	43.6	50.9
TiO_2	0.3	0.3	0.6	2.6	1.7
Al_2O_3	5.6	6.6	9.8	7.9	14.6
Fe_2O_3	1.4	1.5	-	-	-
FeO	9.2	10.2	14.4	21.7	14.6
MnO	0.2	0.2	0.3	0.3	-
MgO	32.0	31.8	18.9	14.9	4.8
CaO	5.3	5.4	8.6	8.3	8.7
Na_2O	0.6	0.03	0.3	0.2	3.1
K_2O	0.03	0.04	0.05	0.05	0.8
P_2O_5	0.03	-	0.2	-	-
H_2O	0.0	0.0	0.0	0.0	0.0
T_{liq} (˚C)	1638	1632	1419	1440	1160
T_{sol} (˚C)	1170	1170	1150	1150	1080
ρ @ T_{liq} (kg/m^3)	2770	2790	2800	2920	2730
ρ @ T_{sol} (kg/m^3)	2860	2890	2860	2980	2740
c (J/kg·˚C)	1780	1780	1640	1573	1470
μ @ T_{liq} (Pa·s)	0.078	0.073	0.81	0.75	86
μ @ T_{sol} (Pa·s)	1.3	1.1	6.9	3.6	230
L @ T_{liq} (J/kg)	6.97E+05	6.94E+05	5.96E+05	5.65E+05	5.37E+05
L @ T_{sol} (J/kg)	4.74E+05	4.74E+05	4.74E+05	4.74E+05	5.03E+05
Reference	1	2	3	4	5

Notes: Liquidus temperatures (T_{liq}) were calculated using MELTS (Ghiorso and Sack, 1995); the solidus temperature (T_{sol}) for komatiite is from Arndt (1976) and is estimated for komatiitic basalt and tholeiitic basalt. Liquid density (_) was calculated using the method of Bottinga and Weill (1970); liquid viscosity (_) was calculated using the method of Shaw (1972); specific heat (c) was calculated from the heat capacity data of Lange and Navrotsky (1992); and heat of fusion (L) for komatiite liquids is approximated using the expression for forsterite of Navrotsky (1995) and for komatiitic and tholeiitic basalt liquids is approximated using the expression for diopside of Stebbins et al. (1983).

References: (1) Kambalda komatiite (adapted from Lesher and Arndt, 1995); (2) Perseverance komatiite WAP111-449 (Barnes et al., 1995); (3) Katinniq komatiitic basalt (Barnes et al., 1982); (4) Apollo 12 sample 12002 (Walker et al., 1976); (5) Columbia River basalt (Murase and McBirney, 1973).

Table 2. Dynamic viscosities of various lavas and analogs at realistic flow temperatures.

Substance	Temperature (°C)	Dynamic Viscosity (Pa·s)	Reference
Distilled Water	25	0.001	1
10W30 Motor Oil	100	0.011	2
Komatiite Lava (33% MgO)	1660	0.024	3
Olive Oil	20	0.082	4
Carbonatite Lava	593	0.3-5.0	5
Lunar Basalt Lava	-	0.4-1	6
Komatiitic Basalt Lava (18% MgO)	1360	1.23	3
Glycerine	15	2.33	7
10W30 Motor Oil	-18	2.4	2
Tholeiitic Basalt Lava	1200	32	8
Mayonnaise	20	100*	9
Tholeiitic Basalt Lava	1150	160	10
Creamy Peanut Butter	20	500*	9
Andesite Lava	1150	1,000	10

*Approximation.

References: (1) Lide (1993); (2) McMillan (1977); (3) Calculated using MELTS (Ghiorso and Sack, 1995); (4) Viswanath and Natarajan (1989); (5) Norton and Pinkerton (1992); (6) Murase and McBirney (1973); (7) Turcotte and Schubert (1982); (8) Shaw (1969); (9) Kokini (1992); (10) Williams and McBirney (1979).

Table 3. Effect on model output due to changes in model input parameters.

Input Parameter	Effect on Maximum Flow Distance	Effect on Thermal Erosion Rate	Effect on Maximum Lava Contamination
Increasing Flow Rate	Increases	Increases	Increases
Superheating Lavas	Decreases	Increases	Strongly Increases
Increasing Ground Slope	Increases	Increases	Slightly Increases
Increasing Lava MgO Content	Increases	Increases	Increases
Increasingly Felsic Substrate	Complex	Complex	Increases
Increasingly Unconsolidated Substrate	Increases	Increases	Increases
Increasingly Hydrous Substrate	Decreases	Increases	Strongly Increases

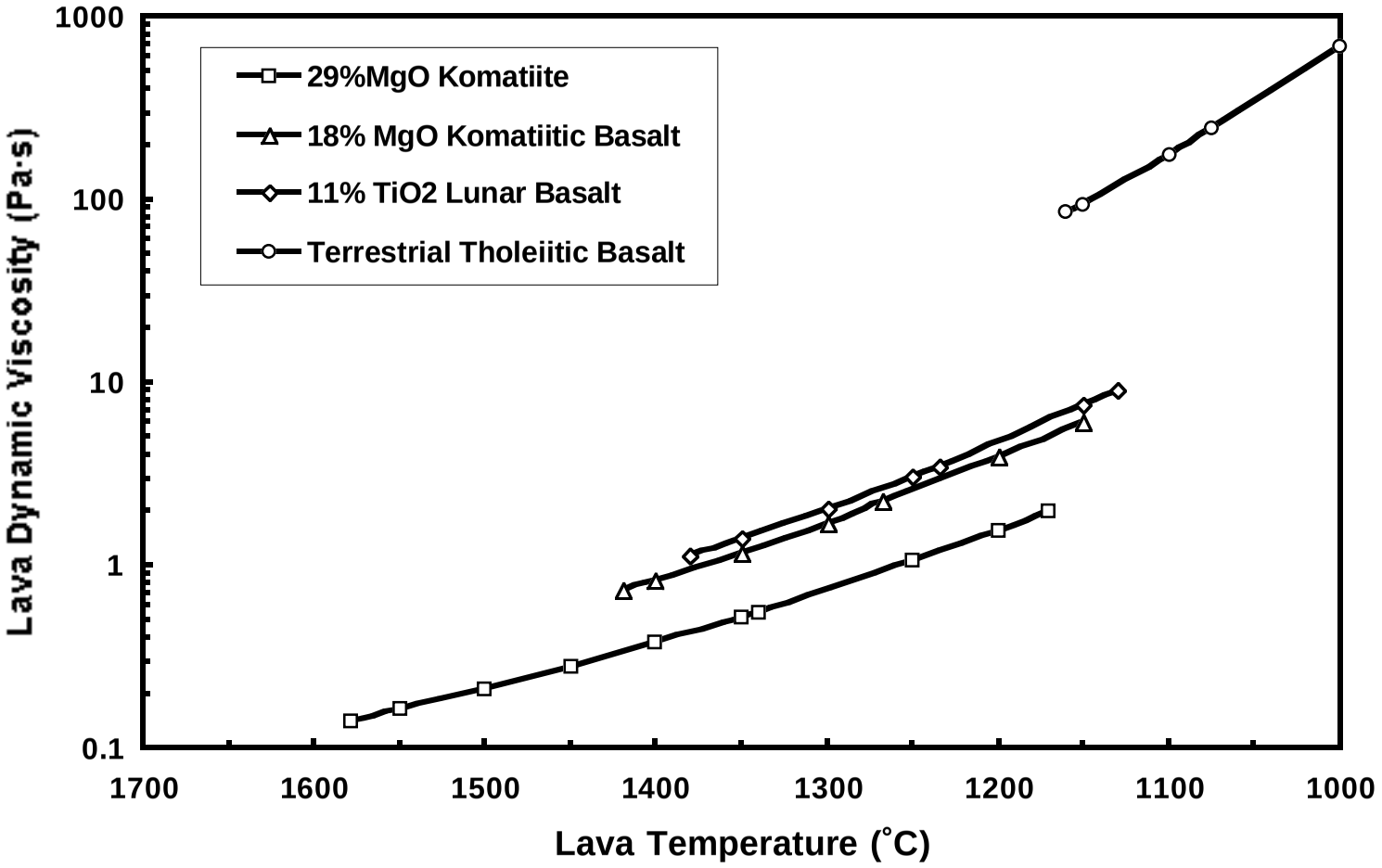
29%MgO Komatiite
18% MgO Komatiitic Basalt
11% TiO2 Lunar Basalt
Terrestrial Tholeiitic Basalt
Lava Dynamic Viscosity (Pa·s)
1000
100
10
1
0.1
1700
1600
1500
1400
1300
1200
1100
1000
Lava Temperature (˚C)

Figure 1.

Figure 2.

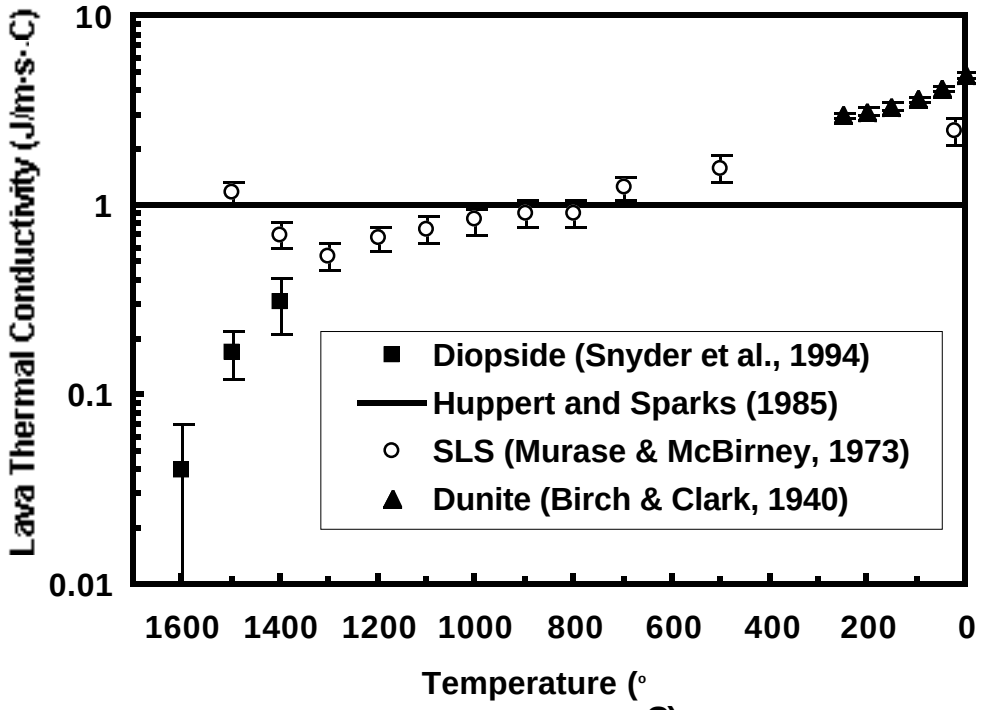
Lava Thermal Conductivity (J/m·s·C)
10
1
0.1
0.01
1600 1400 1200 1000 800 600 400 200 0
Temperature (°
Diopside (Snyder et al., 1994)
Huppert and Sparks (1985)
SLS (Murase & McBirney, 1973)
Dunite (Birch & Clark, 1940)

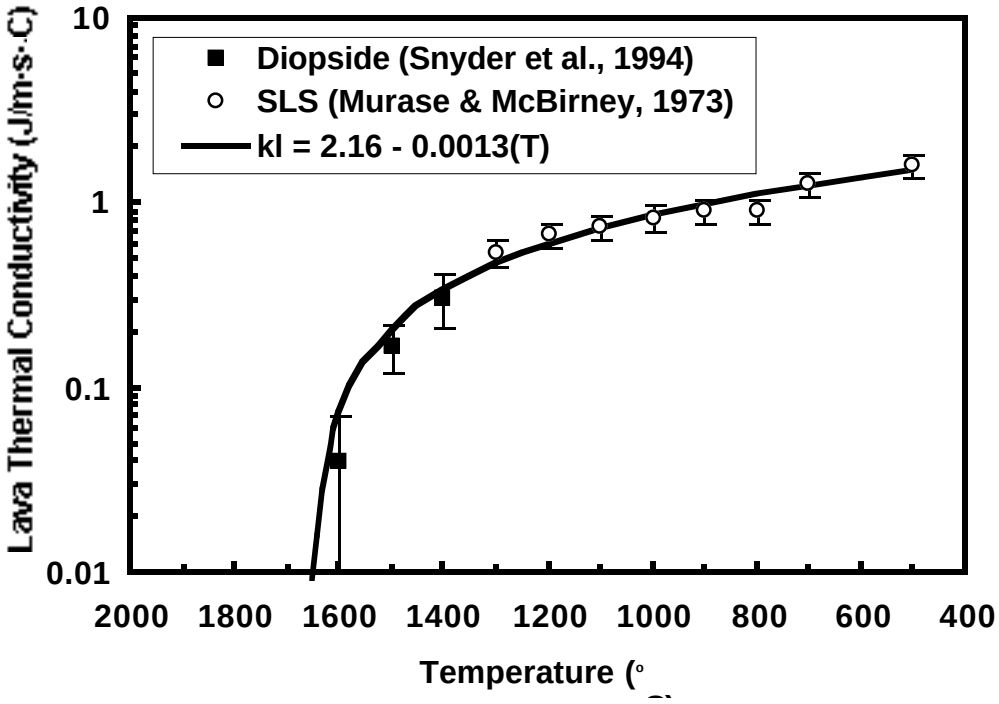
Lava Thermal Conductivity (J/m·s·C)
10
1
0.1
0.01
2000 1800 1600 1400 1200 1000 800 600 400
Temperature (°
Diopside (Snyder et al., 1994)
SLS (Murase & McBirney, 1973)
kl = 2.16 - 0.0013(T)

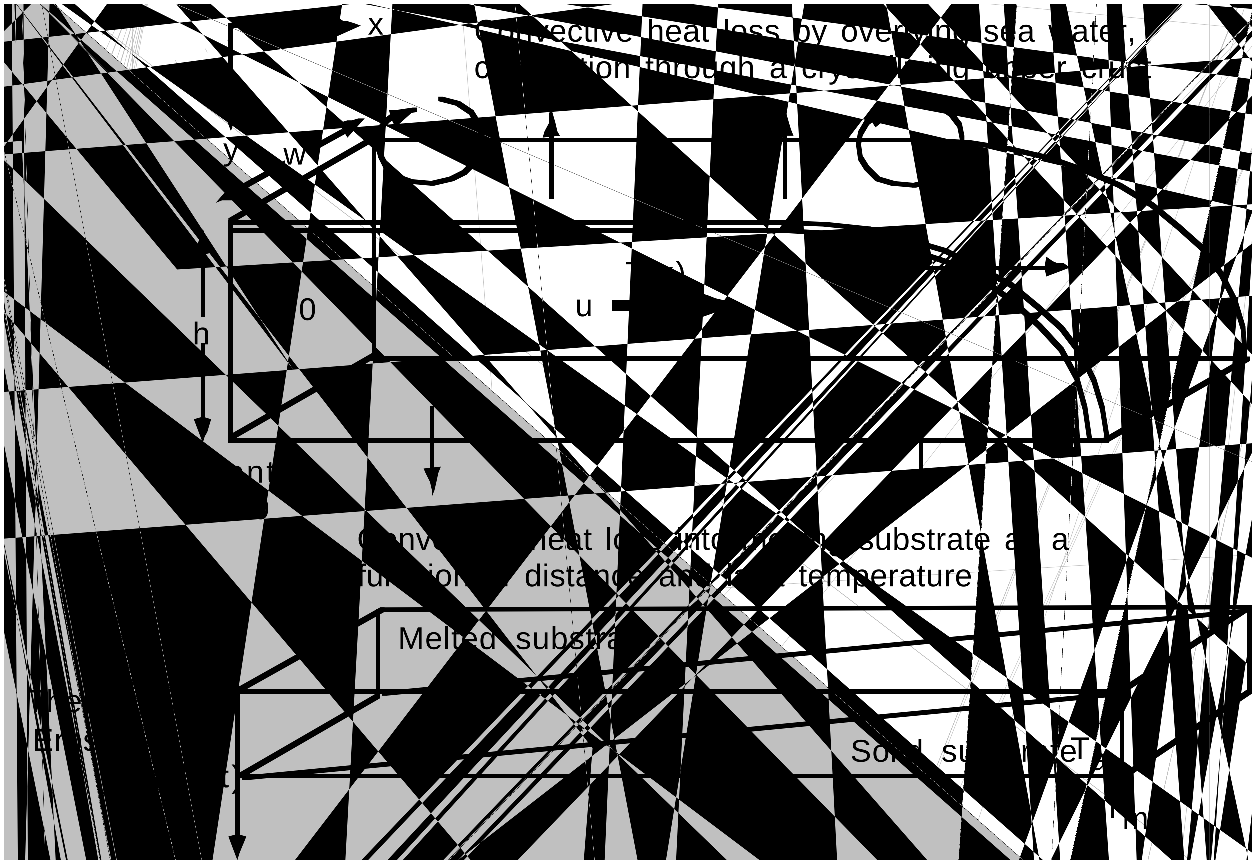

Figure 3.

Figure 4.

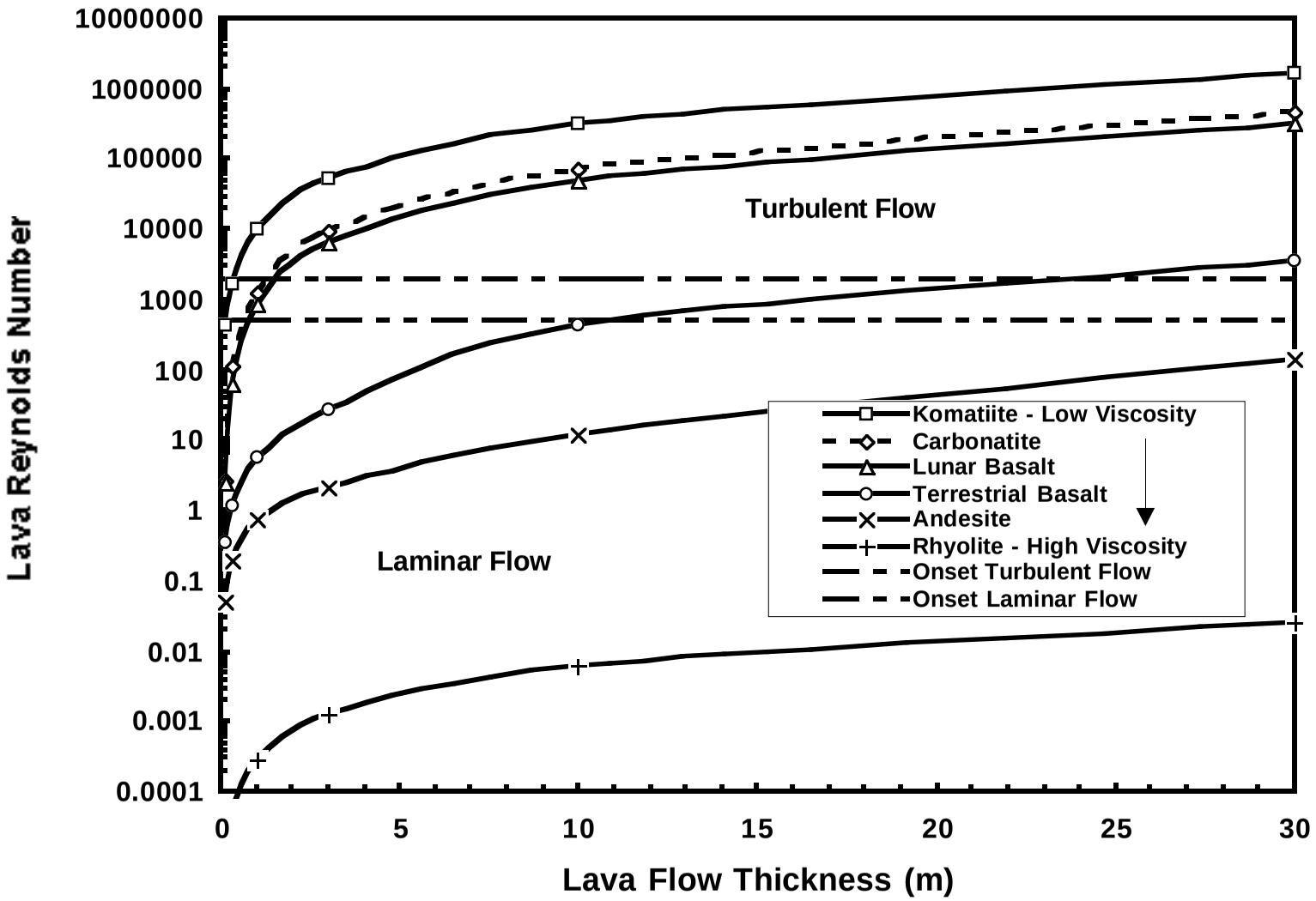
Lava Reynolds Number
10000000
1000000
100000
10000
1000
100
10
1
0.1
0.01
0.001
0.0001
0
5
10
15
20
25
30
Lava Flow Thickness (m)
Turbulent Flow
Laminar Flow
Komatiite - Low Viscosity
Carbonatite
Lunar Basalt
Terrestrial Basalt
Andesite
Rhyolite - High Viscosity
Onset Turbulent Flow
Onset Laminar Flow

Figure 5.

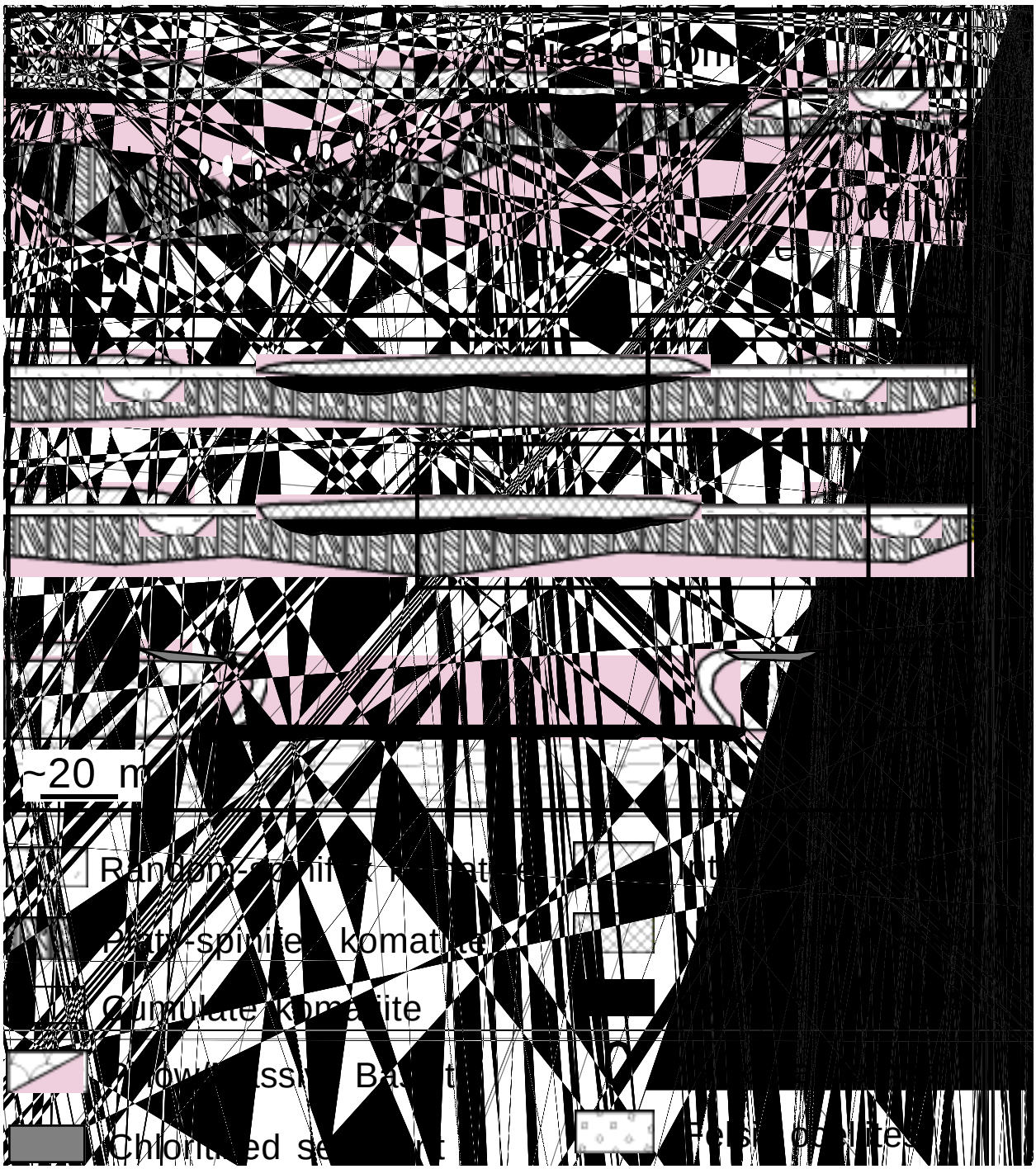

Figure 6.

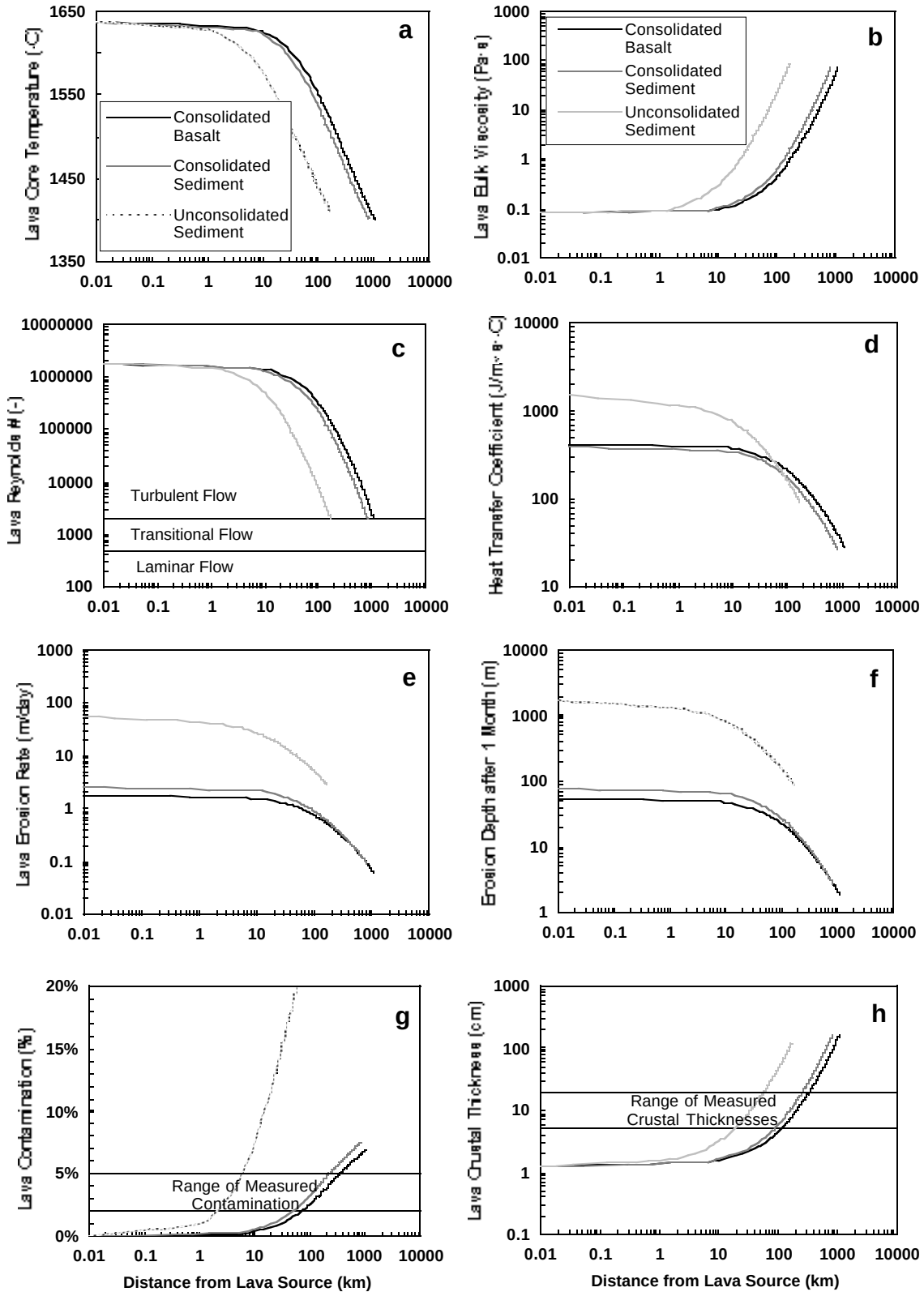
a
Lava Core Temperature (°C)
1650
1550
1450
1350
Consolidated Basalt
Consolidated Sediment
Unconsolidated Sediment
0.01
0.1
1
10
100
1000
10000
b
Lava Bulk Viscosity (Pa·s)
1000
100
10
1
0.1
0.01
Consolidated Basalt
Consolidated Sediment
Unconsolidated Sediment
c
Lava Reynolds # (-)
10000000
1000000
100000
10000
1000
100
Turbulent Flow
Transitional Flow
Laminar Flow
d
Heat Transfer Coefficient (J/m²·s·°C)
10000
1000
100
10
e
Lava Erosion Rate (m/day)
1000
100
10
1
0.1
0.01
f
Erosion Depth after 1 Month (m)
10000
1000
100
10
1
g
Lava Contamination (%)
20%
15%
10%
5%
0%
Range of Measured Contamination
Distance from Lava Source (km)
h
Lava Crustal Thickness (cm)
1000
100
10
1
0.1
Range of Measured Crustal Thicknesses
Distance from Lava Source (km)

Figure 7.

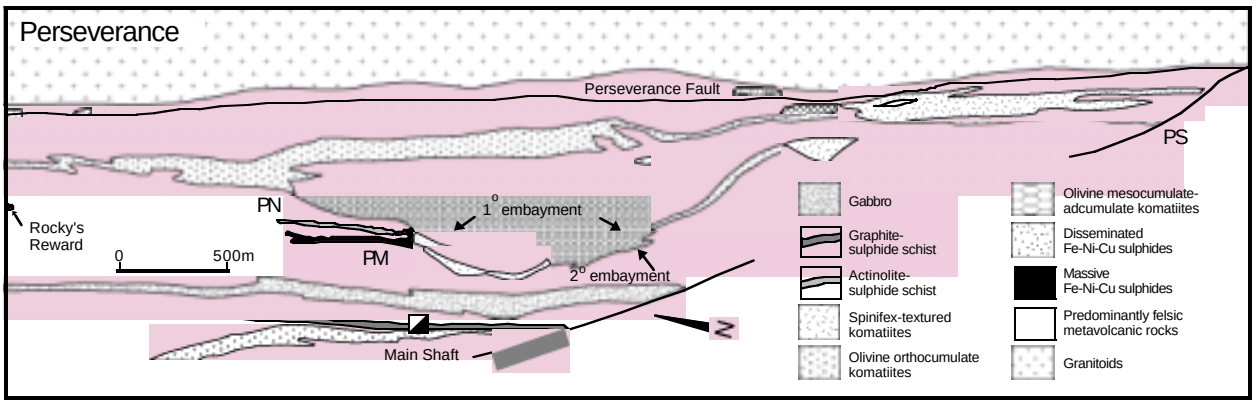
Perseverance
Perseverance Fault
PS
PN
PM
1° embayment
2° embayment
Rocky's Reward
0
500m
Main Shaft
N
Gabbro
Graphite-sulphide schist
Actinolite-sulphide schist
Spinifex-textured komatiites
Olivine orthocumulate komatiites
Olivine mesocumulate-adcumulate komatiites
Disseminated Fe-Ni-Cu sulphides
Massive Fe-Ni-Cu sulphides
Predominantly felsic metavolcanic rocks
Granitoids

Figure 8a. Superheated Lava over partly-consolidated (welded) , hydrous tuff.

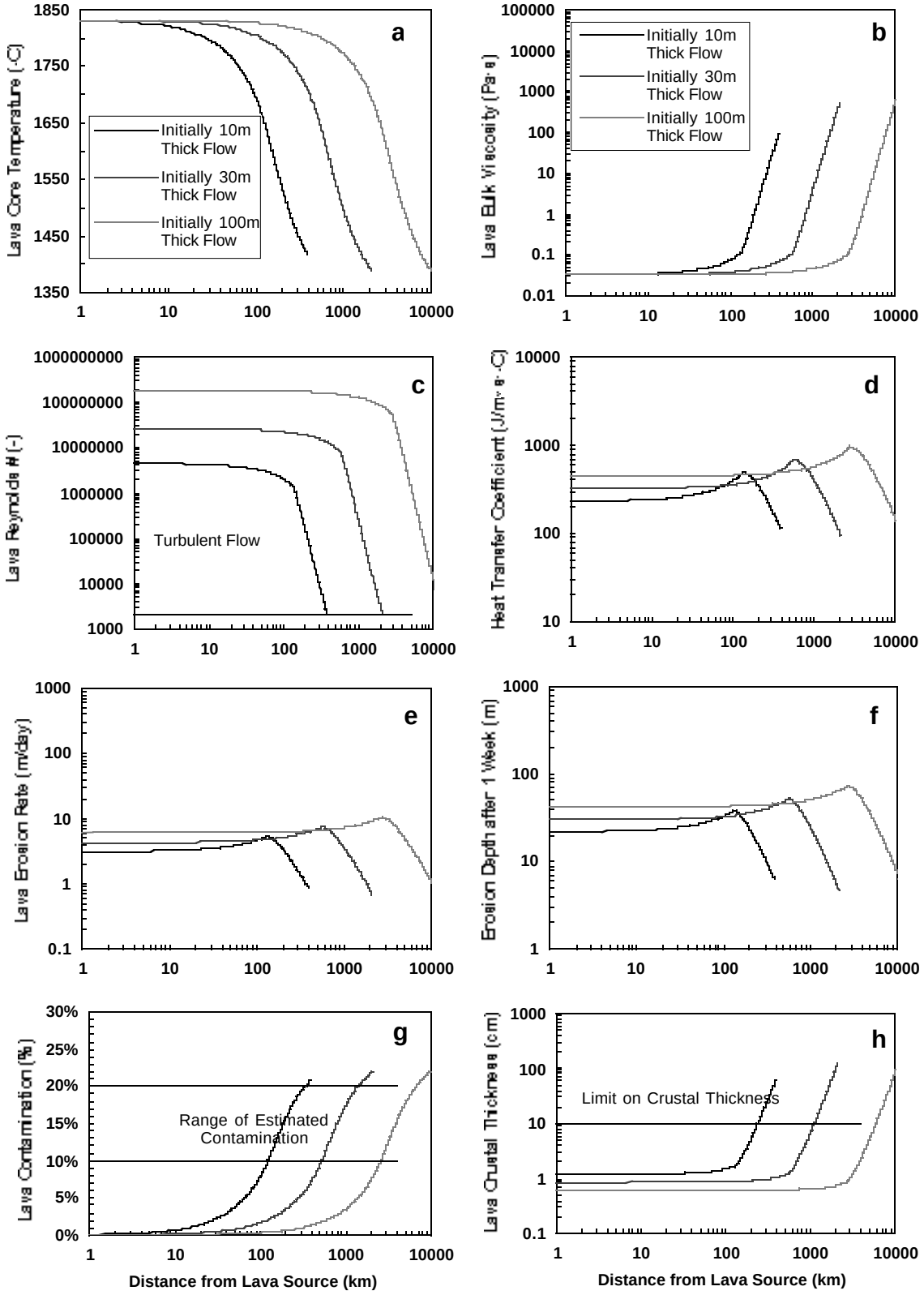

Figure 8b. Non-superheated lava over unconsolidated, hydrous tuff.

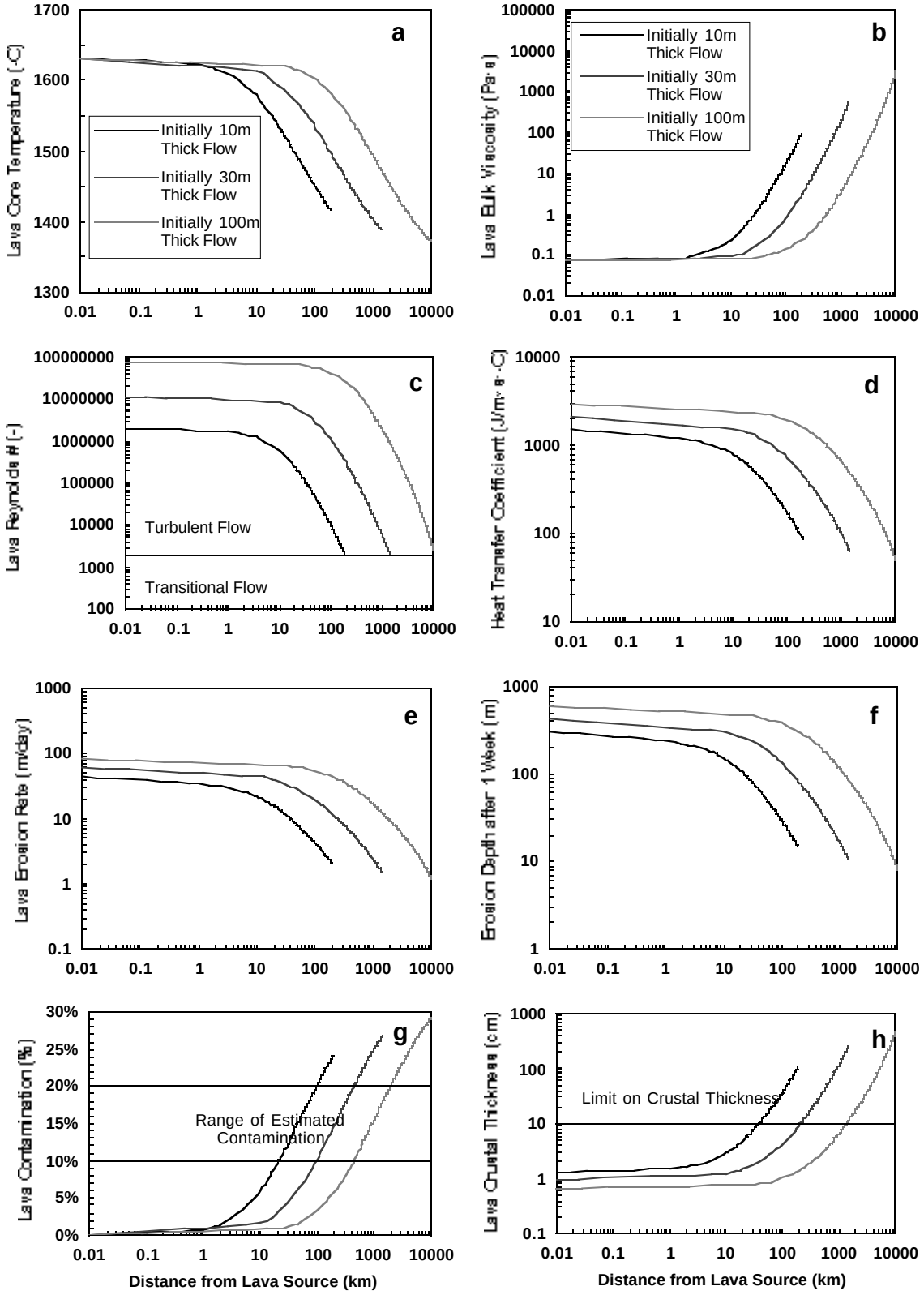

Figure 9.

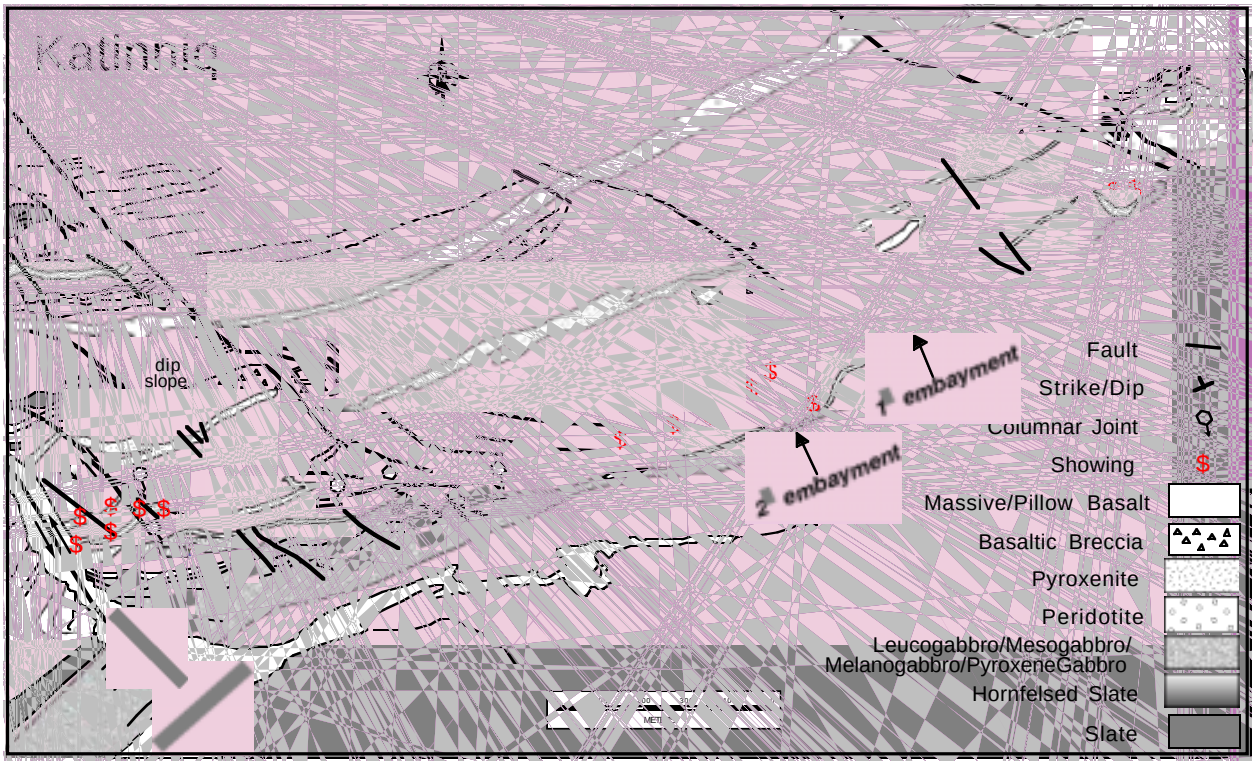
dip
slope
embayment
embayment
Fault
Strike/Dip
Columnar Joint
Showing
Massive/Pillow Basalt
Basaltic Breccia
Pyroxenite
Peridotite
Leucogabbro/Mesogabbro/
Melanogabbro/PyroxeneGabbro
Hornfelsed Slate
Slate
N
MET

Figure 10a.

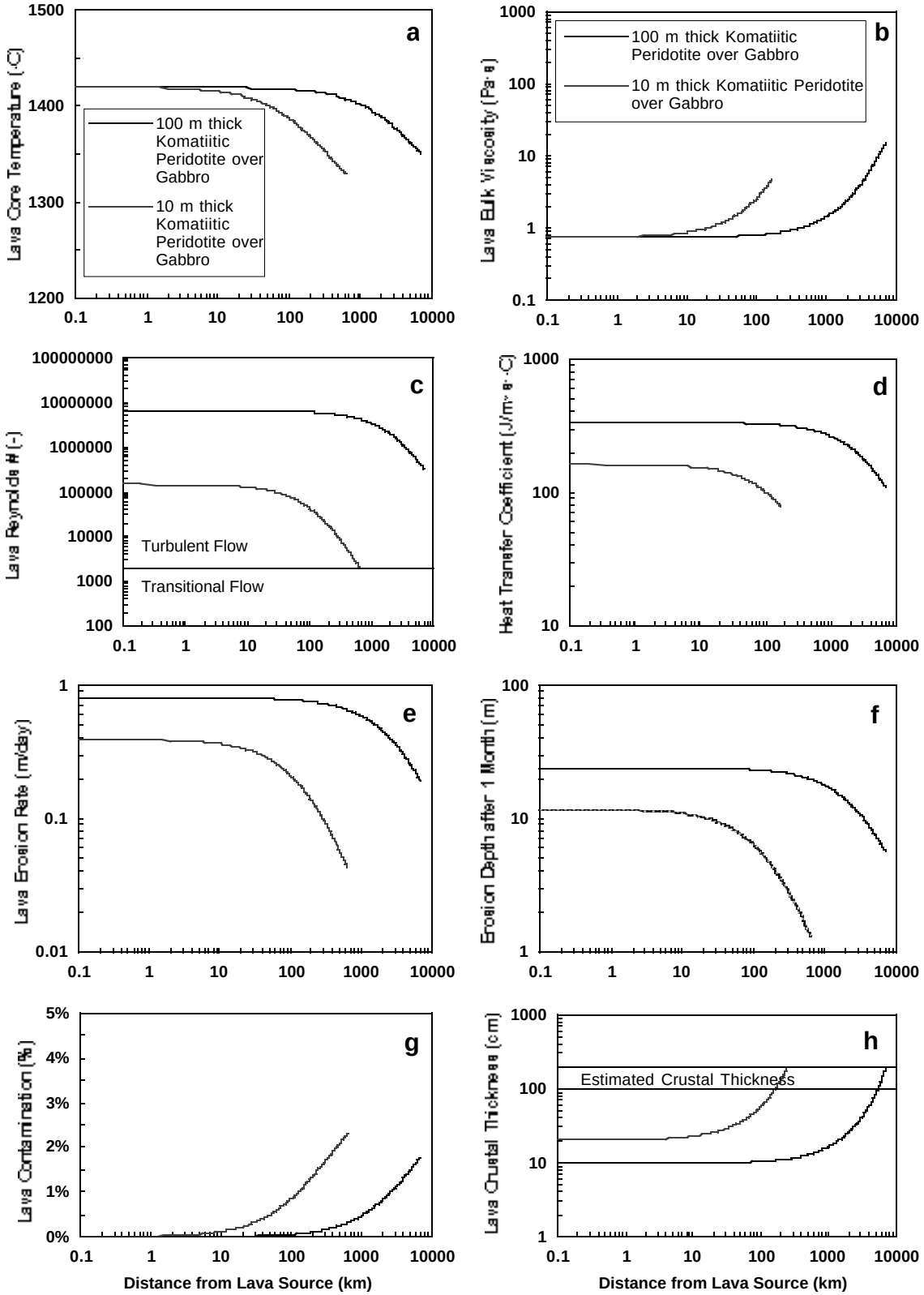
a
Lava Core Temperature (°C)
1500
1400
1300
1200
100 m thick Komatiitic Peridotite over Gabbro
10 m thick Komatiitic Peridotite over Gabbro
b
Lava Bulk Viscosity (Pa s)
1000
100
10
1
0.1
100 m thick Komatiitic Peridotite over Gabbro
10 m thick Komatiitic Peridotite over Gabbro
c
Lava Reynolds # (-)
100000000
10000000
1000000
100000
10000
1000
100
Turbulent Flow
Transitional Flow
d
Heat Transfer Coefficient (J/m² s °C)
1000
100
10
e
Lava Erosion Rate (m/day)
1
0.1
0.01
f
Erosion Depth after 1 Month (m)
100
10
1
g
Lava Contamination (%)
5%
4%
3%
2%
1%
0%
h
Lava Crustal Thickness (cm)
1000
100
10
1
Estimated Crustal Thickness
0.1
1
10
100
1000
10000
Distance from Lava Source (km)
Distance from Lava Source (km)

Figure 10b.

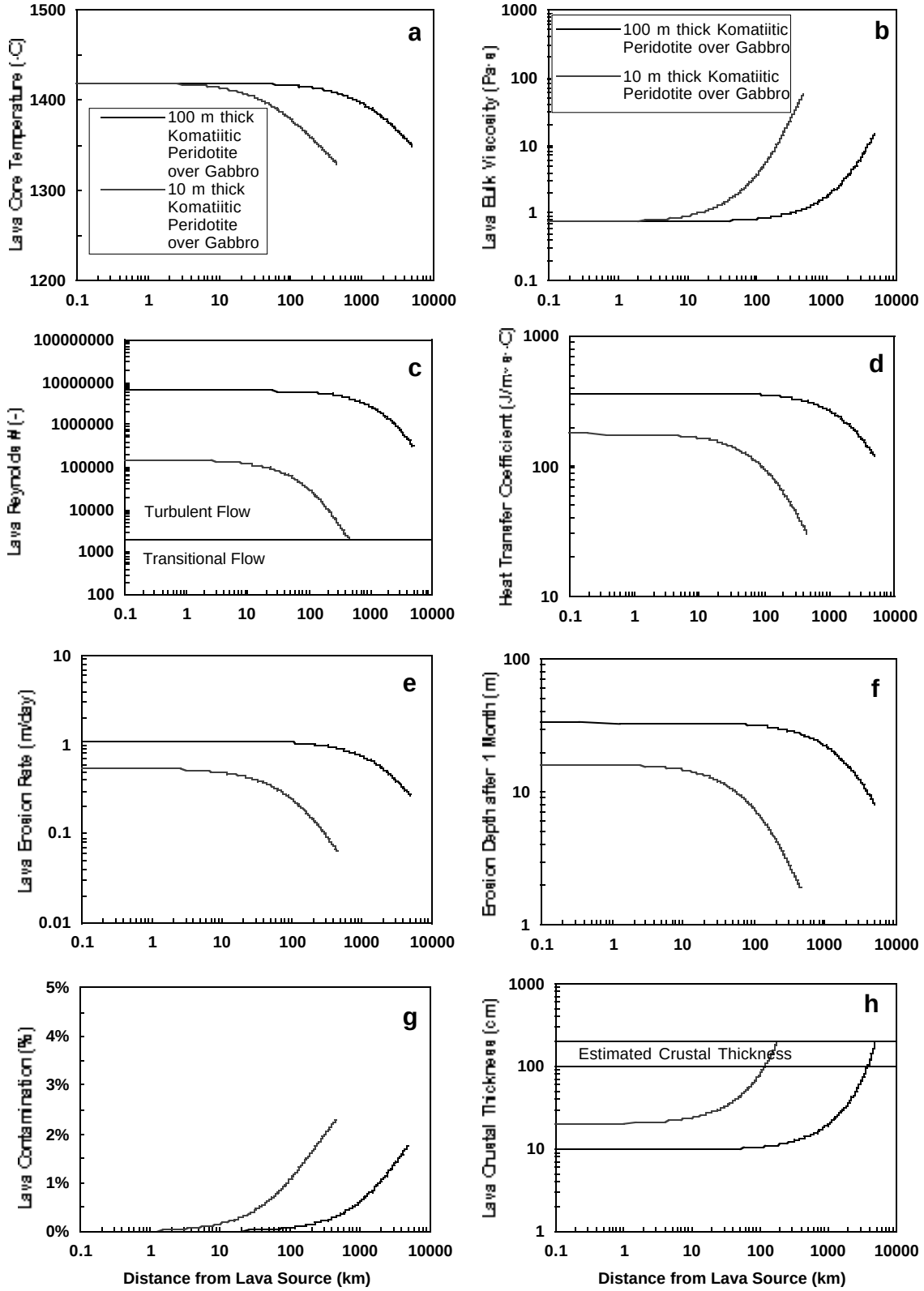
a
Lava Core Temperature (°C)
1500
1400
1300
1200
100 m thick Komatiitic Peridotite over Gabbro
10 m thick Komatiitic Peridotite over Gabbro
b
Lava Bulk Viscosity (Pa·s)
1000
100
10
1
0.1
100 m thick Komatiitic Peridotite over Gabbro
10 m thick Komatiitic Peridotite over Gabbro
c
Lava Reynolds # (-)
100000000
10000000
1000000
100000
10000
1000
100
Turbulent Flow
Transitional Flow
d
Heat Transfer Coefficient (J/m²·s·°C)
1000
100
10
e
Lava Erosion Rate (m/day)
10
1
0.1
0.01
f
Erosion Depth after 1 Month (m)
100
10
1
g
Lava Contamination (%)
5%
4%
3%
2%
1%
0%
Distance from Lava Source (km)
h
Lava Crustal Thickness (cm)
1000
100
10
1
Estimated Crustal Thickness
Distance from Lava Source (km)
0.1
1
10
100
1000
10000

Figure 10c.

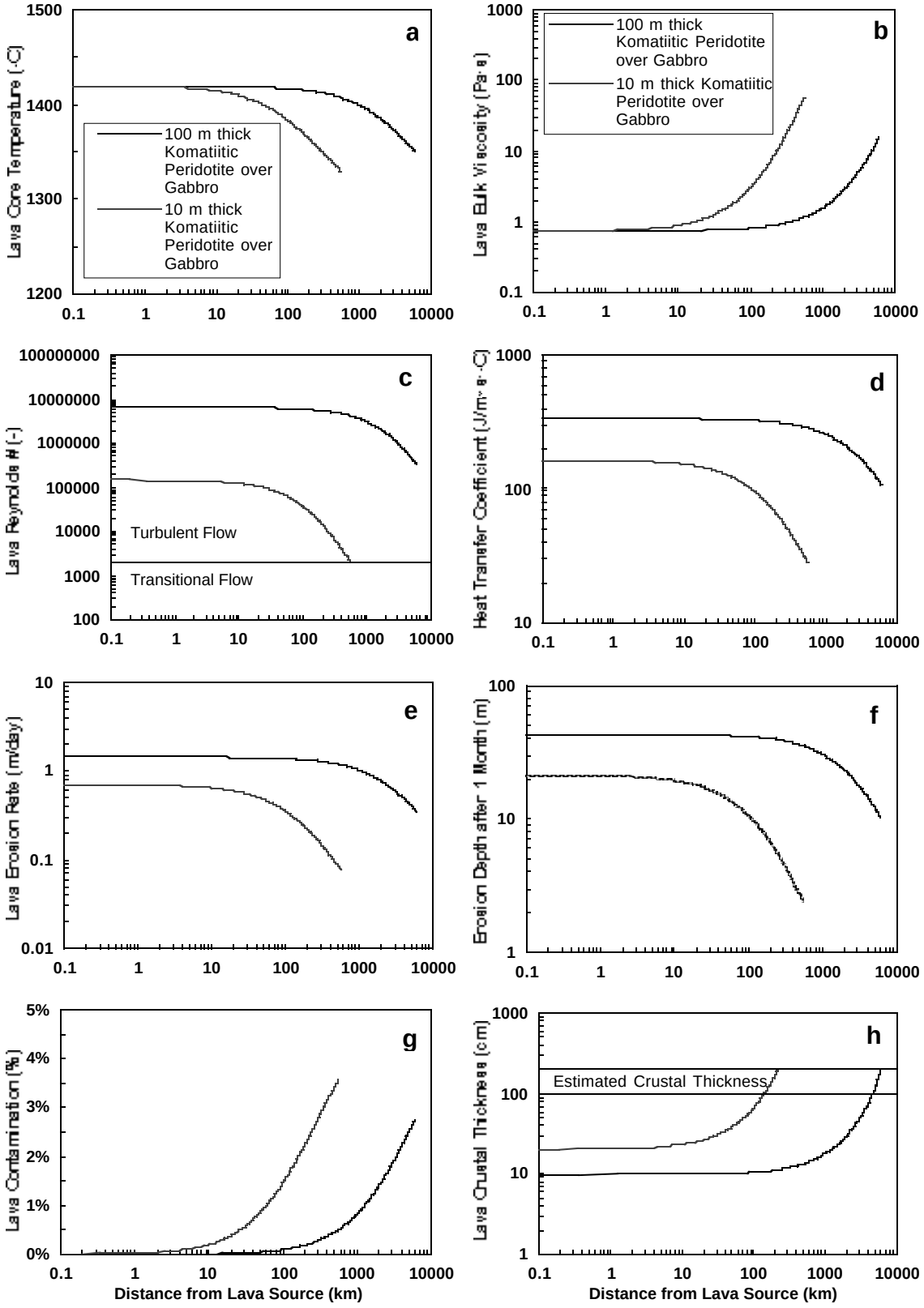
a
Lava Core Temperature (°C)
1500
1400
1300
1200
100 m thick Komatiitic Peridotite over Gabbro
10 m thick Komatiitic Peridotite over Gabbro
0.1
1
10
100
1000
10000
b
Lava Bulk Viscosity (Pa·s)
1000
100
10
1
0.1
100 m thick Komatiitic Peridotite over Gabbro
10 m thick Komatiitic Peridotite over Gabbro
c
Lava Reynolds # (-)
100000000
10000000
1000000
100000
10000
1000
100
Turbulent Flow
Transitional Flow
d
Heat Transfer Coefficient (J/m²·s·°C)
1000
100
10
e
Lava Erosion Rate (m/day)
10
1
0.1
0.01
f
Erosion Depth after 1 Month (m)
100
10
1
g
Lava Contamination (%)
5%
4%
3%
2%
1%
0%
Distance from Lava Source (km)
h
Lava Crustal Thickness (cm)
1000
100
10
1
Estimated Crustal Thickness
Distance from Lava Source (km)

Figure 11.

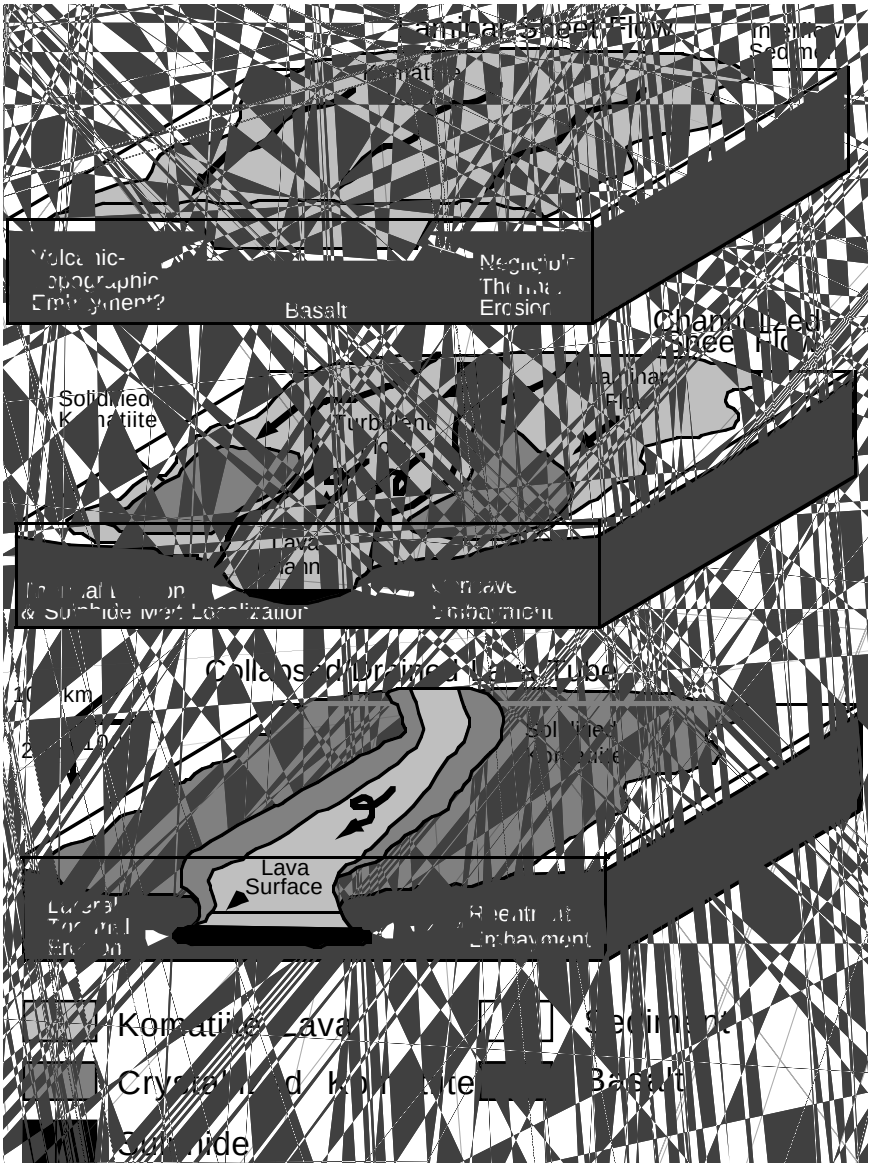
Basalt
Lava Surface
Komatiite Lava
Sediment
Basalt
Sulfide